PRESIDENCY UNIVERSITY

DEPARTMENT OF LIFE SCIENCES

Submission of 5000 Words synopsis

Title- Structural and Biochemical characterization of a class III sirtuin, OsCobB in *Oryza sativa indica* and its association to stress response in plants

Sonali Khan

Ph.D. Registration No. - R-19RS218210261

Date – 28th July, 2021

Supervisor – Dr. Sanghamitra Dey

Department of Life Sciences

Presidency University

Kolkata- 700073, West Bengal, India

Synopsis (5000 words)

Name:	Sonali Khan
Supervisor:	Dr. Sanghamitra Dey
Title of Thesis:	Structural and biochemical characterization of a class III sirtuin, OsCobB in *Oryza sativa indica* and its association to stress response in plants
PhD registration Number with date:	R-19RS218210261, 28th July, 2021
Enrolment Number with date:	PU/PHD/DLS/2019/081, 2nd January, 2020
Place of work:	Presidency University, Kolkata
Residential Address:	No 1 Ukilpara, Po-Raiganj, Dist- Uttar Dinajpur, West Bengal-733134
Corresponding Address:	Anand Vihar Apartment, phase II, Block A, 25, Nagendranath road, satgachi, Kolkata-700028
Email:	sonali.khan.03@gmail.com
Phone Number:	8902774785

Forwarded

Sonali Khan

Signature of Research Scholar

Dr. Sanghamitra Dey
Assistant Professor of Biochemistry
Department of Life Sciences
Presidency University, Kolkata

Signature of Supervisor

Contents

Sr. no.	Objective	Page no.
1.	Abstract	4-5
2.	Introduction	5-7
3.	Objectives	7-8
4.	Methodology	8-13
5.	Results and Discussion	13- 40
	Objective 1- *In-silico* studies to understand the molecular mechanism of OsCobB	13-22
	Objective 2- Determination of the possible enzyme activity and its regulation in plants	22- 34
	Objective 3- Insight into the biological significance of the protein under stress conditions.	34- 40
6.	Conclusion	40-41
7.	Future directions	41-42
8.	Reference	42- 46
9.	Plagiarism Certificate	47
10.	Appendix	48- 53

1. Abstract

Protein posttranslational modifications (PTMs) by lysine acylation are unfolding as a channel of metabolic regulations in response to critical environmental stress conditions. Sirtuins are the NAD^+- dependent deacylases that have been well-researched to play an important role in these PTMs in organisms ranging from prokaryotes to eukaryotes. However, plant sirtuins are still a lesser explored area. This work focuses on OsCobB that has been identified in *Oryza sativa var indica* as the only member of class III sirtuin family in plants. Besides, this protein has 89% sequence identity with the bacterial sirtuin, CobB. Thus, it would be interesting to explore the structural and biochemical aspects of a CobB-like protein in plants to better understand its biological roles. OsCobB is localized majorly in the mitochondria with traces present in the nucleus as well, depending on its deacylase activity under stress conditions. Histones H3 and H4 are the nuclear targets for OsCobB, with a preference of deacetylation at H3K9 and H3K18 residues. Molecular simulation studies have confirmed that NAD^+ binding is a pre-requisite for the effective binding of the substrate at the active site of OsCobB. The formation of a hydrophobic tunnel at the catalytic site is necessary for the proper incorporation of the acyl modification which would otherwise be loosely bound to the protein. Additionally, molecular docking analysis with H3K9 peptide linked to varied acylations predicted its preference of binding with succinyl, malonyl and glutaryl groups effectively. There is also a possibility of conformational changes at the active site for the incorporation of longer acyl side chains. This was further supported by *in-vitro* deacylase experiments with OsCobB. The interaction between the lysine modifications and Tyr55 and Arg58 residues of the protein strengthens the binding of the negatively charged acyl groups. No ADP ribosyl transferase activity was detected in OsCobB, in contrast to some of the class III members. The deacetylation of histone H3 was unstirred by its products, nicotinamide and ADP ribose but was sensitive to metal ions like Mg^{2+} and Fe^{2+}. A rise in nuclear OsCobB expression was noted during low temperature and dehydration conditions. This can be associated to increased H3 and H4 desuccinylation during cold stress and increased H4 desuccinylation and H3 debutrylation during low water availability. In mitochondria, Isocitrate dehydrogenase (IDH2) was a target for deacetylation and desuccinylation at K391. IDH2 activity increased 2-fold in the presence of OsCobB which may have a pivotal role in responding to dehydration and low temperature stress. Surprisingly, Acetyl CoA Synthetase (ACS) was also found to be a substrate for OsCobB in both mitochondria and

nucleus, capable of deacetylation as well as desuccinylation of the target. Additionally, mitochondrial ACS activity increased by 2-fold while the activity of nuclear ACS increased by 3-fold in the presence of OsCobB. This regulation might have a role to play in the nucleus by increased desuccinylation of ACS during high saline conditions by overexpressed OsCobB. Incidentally, under this stress condition, OsCobB is downregulated in the mitochondria. Thus, we found a correlation between removal of lysine modifications from the substrate and overexpressed OsCobB under different plant stresses that can be hypothesized to play a role in evading the stress. In this way, our study is the first to characterize the different deacylations by OsCobB in *O.sativa var indica*, both *in-vivo* as well as *in-vitro*.

2. Introduction

Sirtuins belong to class III HDAC superfamily with NAD^+-dependent deacylase and/or ADP ribosyltransferse activity, regulating the functioning of numerous potential targets[1–3]. The acyl moiety on the substrate lysine side chain is transferred to NAD^+ to produce nicotinamide (NAM), 2'-O-acetyl-ADP-ribose and the deacylated substrate in the process. In the past years, a number of post translational modifications (PTMs) have been brought to light[4–8]. These modifications are found on histones as well as non-histone proteins, indicating a wider distribution in cells and having decisive role in its physiological functioning [4,8–13]. Although the influence of their structural distinctions needs further explorations in context to various metabolic pathways under different stress conditions.

Based on amino acid sequences, sirtuins are grouped into 5 classes- (class I-IV and U)[1].Mammalian sirtuins, SIRT1, SIRT2 and SIRT3, together with yeast sirtuin proteins, Hst1 and Hst2, belong to class I[1,2]. They are majorly responsible for deacetylation of its substrates. SIRT1 is capable of directly deacetylating several transcription factors like the tumor suppressor protein, p53, impacting aging related diseases in mammals[14]. SIRT2 and SIRT3 deacetylases play a role in DNA homologous recombination repair[15]. Although, recently, SIRT1, SIRT2 and SIRT3 have been found to catalyze the decrotonylation of histone H3, in turn regulating gene transcription as Kcr are mostly enriched at promoter sites[16]. The mammalian sirtuin, SIRT4, belong to class II, showing detectable ADP ribosyltransferase activity with poor deacetylation[1,2]. Of late, SIRT4 has also been shown to possess lipoamidase abilities inhibiting pyruvate dehydrogenase complex (PDH) activity controlling the pyruvate decarboxylase levels during

glycolysis[17]. Almost all bacterial sirtuins belong to class III. *E.coli* CobB has been previously reported to exhibit lysine desuccinylase, deacetylase and 2-hydroxyisobutryltransferase activities[18–20]. The chemotaxis mechanism in bacteria is controlled reversibly by CobB[21]. Bacterial sirtuins also play a vital role in short chain fatty acid biosynthesis in *Salmonella typhimurium* and *Bacillus subtillis*[22–24]. Mammalian sirtuin, SIRT5 also belongs to class III along with the fungal sirtuin in *Candida albicans*, Hos2, archeal sirtuin in *Archaeoglobus fulgidus*, Sir2Af1 and Sir2Af2, and protozoan sirtuin in *Plasmodium falciparum*, PfSir2A[1,25–27]. SIRT5 features a weak deacetylase activity, displaying a more prominent desuccinylase, demalonylase and deglutarylase abilities[12,26,28]. Class IV sirtuins include mammalian sirtuins, SIRT6 and SIRT7[1]. SIRT6 is known to hydrolyse long chain fatty acids efficiently while its deacetylase activity is specific to H3K9 and H3K56 peptides only[29,30]. Studies in the recent past has revealed the implications of SIRT6 in lipid metabolism, having a therapeutic advantage in treatment of numerous fatty liver diseases[31]. It also plays a role in suppressing cellular senescence in mammals[32,33]. Notably, SIRT7 showed detectable deacetylase, desuccinylase, debutrylase, decrotonylase and ADP-ribosyltransferase activities[34–37]. SIRT7 is involved in deacetylation of H3K18 and in turn promotes transcription repression controlling tumour growth[34]. Class U sirtuins comprise of the undifferentiated sirtuins with sequence motifs that are intermediate between class II and III and class I and IV. *Thermatoga maritima* and several gram positive bacterial sirtuins like *Streptomyces coelicolor A3* (*S.coe2*) and *Staphylococcus aureus* fall under this category of class U sirtuins.

Sirtuins have been discovered in plants as well but there are limited reports on sirtuin-catalyzed kinetics or deacylase activities and the biological significance of the acylations. Plant sirtuins are familiar to provide protective shielding against genome fluidity and oxidative damage protection, requisite for proper cell growth along with maturation and ripening of fruits and modulation of photosynthesis and plant hormonal signaling pathways. In *Vitis vinifera*, VvSRT1 is nuclear localized and plays a vital role in plant development and growth. VvSRT2, on the other hand, is localized in both mitochondria and chloroplast and it plays its part in gene transcription regulation in association with leaf senescence and photosynthesis[38]. *Arabidopsis thaliana* also has 2 sirtuins, AtSRT1 and AtSRT2[39]. AtSRT1 is localized in the nucleus and is responsible for auxin signaling. AtSRT2, which is found to colocalize in both nucleus and mitochondria, acts as a negative regulator in plant defense mechanism involving PAD4 (phytoalexin deficient 4), SID2

(salicylic acid induction deficient) and EDSS (enhanced disease susceptibility)[39]. SoSRT1 and SoSRT2 are the two sirtuins in *Solanum lycopersicum*[40]. Both the sirtuins are localized in the nucleus, while SoSRT2 was detected in the cytoplasm as well. *Glycine max*, on the other hand, has 4 sirtuins (GmSRT1, GmSRT2, GmSRT3 and GmSRT4) whose biological roles have not been discovered yet[41].

No class III sirtuin has been reported in plants till this study. OsCobB in *Oryza sativa var indica* is the first reported sirtuin protein with deacylase activity in this class. The other rice sirtuins, OsSRT1 and OsSRT2 in *O.sativa* belong to class IV and class II based on their sequence alignment[42,43]. OsSRT1 is nuclear localized. It is required to protect against cell damage in oxidative stress conditions[43,44]. OsSRT2, on the other hand, is a mitochondrial protein with decrotonylase activity[45]. So it would be interesting to know the function and regulation of a class III protein in plants. Since class III sirtuins have been reported to be involved in numerous deacylation activities, we have explored the same for OsCobB in this study. Further we have correlated its role in relation to substrate deacylation with the intent of exploring its biological implications in rice. This would give an opportunity for future biological studies of these deacylations in plant physiology and functioning. Further, we have also inspected the regulation of OsCobB in this study.

3. Objectives

1. *In-silico* studies to understand the molecular mechanism of OsCobB
    a. Structural characterization of OsCobB.
    b. Comparative phylogenetic analysis and identification of the conserved motifs required for its acylation activities.
    c. Molecular simulation and docking studies to determine the possible bioactive conformations of its substrates.
2. Determination of the possible enzyme activity and its regulation in plants
    a. Identification of its subcellular localization.
    b. *In-vitro* OsCobB catalyzed deacylation studies and comparative analysis of its kinetic parameters among members of class III sirtuins.

c. Exploration of the regulatory mechanism in OsCobB-associated deacylation processes.

3. Insight into the biological significance of the protein under stress conditions.

4. Methodology

The reagents used for this work was purchased from Sisco Research Laboratories (SRL) India, HiMedia laboratory, India and Sigma-Aldrich, USA. Primers were synthesized from IDT DNA, USA. Taq DNA polymerase, restriction enzymes (*BamHI* and *NcoI)* and T4 DNA ligase were obtained from New England Biolabs, USA.

4.1 *In-silico* studies and molecular docking analysis

The three-dimensional structure of OsCobB was prepared after downloading the amino acid sequence from NCBI (OsI_09569) and then the structure was predicted using Swiss-model (https://swissmodel.expasy.org/). A homology search of protein database at NCBI (National Center for Biotechnology Information) with OsCobB helped in identifying proteins with higher sequence similarity. ClustalW and Espript 3.0 were used to align different sirtuins and analyze their sequence motifs in order to classify OsCobB into its sirtuins class. Computational Docking was performed using Autodock Vina by employing different acyl modifications at the substrate binding site to acquire possible orientation of the acyl modification. The protein-ligand complexes were then subjected to molecular dynamics simulation studies using GROMACS (2019.4). The pdb files, thus, generated were analyzed using Chimera UCSF 1.16 and Ligplot+ v.1.4.5 softwares to understand the molecular interactions between OsCobB-ligand complexes. Molecular phylogeny of sirtuins was analyzed using phylogenetic analysis software, Mega 11.0 using the maximum likelihood (ML) method. The bootstrap values in the rooted phylogram estimates the relatedness of the species in the phylogenetic tree.

4.2 Rice plant growth conditions

The rice seeds of IR64 and Swarna varieties as well as pathogen and low temperature stress were obtained from authorized vendors. Whole grown plants of drought varieties were obtained from local rice fields. All seeds were surface sterilized and grown in the dark for 48hrs for germination. Post germination, they were transferred to phyta jars containing hydroponics solution (Murashige and Skoog media) and were grown at 25°C with 10 h white light/14 h dark photoperiod for about 3 weeks till the rice plant grows to 3-leaf stage. For inducing different stresses, 3-week grown rice plants were supplemented with heavy concentrations of metal salts in the media. For exposing plants to dehydration stress conditions, the 3 week old plants were taken out of the hydroponics solution for 2 days. All the plant samples were flash frozen and stored at −80°C.

4.3. Subcellular organellar protein extraction from rice leaves

Protein extraction were carried out using a modified protocol of Abcam cell fractionation kit (ab109719) using 5g leaves. They were crushed in detergent 1: buffer A solution and centrifuged as indicated in the kit to obtain the cytoplasmic proteins in the supernatant fraction. The pellet was further washed multiple times in buffer A by spinning at 6000 to 13,000×g. The supernatants were collected after each of the spins and western blot analyses were carried out with compartment specific antibody markers to locate the organellar proteins. The supernatant from 7000×g spin contained most of the chloroplast proteins. The pellet obtained from the 13000xg spin was then resolubilized and centrifuged as per the protocol in the kit to obtain enriched mitochondrial protein. The final pellet was resuspended in 250µL RIPA buffer (10 mM Tris-HCl (pH 8.0), 150 mM NaCl, 1 mM EDTA, 1% Triton X-100, 0.1% SDS and 1 mM PMSF) and centrifuged at 10,000×g. The supernatant obtained contained the enriched nuclear protein. All the samples (20µg) were analyzed using western blot. Nuclear, chloroplast, mitochondrial and cytoplasmic extracts were verified using compartment specific antibody markers. Extracts from stressed plant varieties were also obtained using the same protocol.

4.4. Analysis of OsCobB expression in different tissues of the rice plant

Rice plants grown to different developmental stages were used to extract proteins from different plant parts. 2 g each of the plant parts were grounded in liquid nitrogen. 1 ml of hypotonic solution (10 mM Tris-HCl (pH 8.0), 1 mM KCl, 1mM MgCl2, 1 mM DTT and 1 mM PMSF) was added to each of these samples to promote osmotic swelling of cells. The mixtures were then centrifuged at 10,000×g and analyzed using western blot analysis using OsCobB specific primary antibody.

4.5. Cloning of OsCobB gene and protein purification of different constructs

The mRNA was isolated from the rice leaves using kit (Himedia-HiPurATM Plant and Fungal RNA Miniprep Purification Kit), followed by cDNA preparation using Invitrogen verso kit. The OsCobB gene (amino acid residues 269–501 of the OsI_09569) was amplified from cDNA using gene specific primers and inserted into pETM30 and modified pET28a vectors between *NcoI* and *BamHI* restriction sites. The modified pET28a vector (for untagged protein) and pETM30 vector (for His-GST tagged protein) containing OsCobB gene were overexpressed in *E.coli* BL21 (DE3) competent cells. Pellet containing His-GST-OsCobB protein was purified utilizing a Ni-NTA column and eluted using imidazole gradient buffer. Cells containing the untagged OsCobB protein was purified utilizing an ion-exchange column (Bio-scale Mini Macro-Prep HighQ Cartridge (Bio-Rad #732–4122)) and eluted using NaCl gradient. Both the proteins were desalted using HiTrap desalting column (Sigma-Aldrich cat # GE17-1408-01) equilibrated with 50 mM phosphate buffer (pH 7.5), 100 mM NaCl, 10% glycerol, 5 mM DTT and 1 mM PMSF.

4.6. *in-vitro* and *in-vivo* interaction studies of OsCobB

1 µg His-GST-OsCobB protein was interacted with 1µg recombinant histones (H3, H4, H1, H2A and H2B) in separate tubes for 2 h along with Ni-NTA beads. The beads were then washed with wash buffer (50 mM phosphate buffer pH 7.5, 300 mM NaCl, 10% glycerol, 1 mM PMSF and 5 mM DTT), and resolved using 12% SDS-PAGE. Similar experiment was carried out to analyze the interaction of OsCobB with mitochondrial proteins, ACS and IDH2 and non-histone nuclear protein, ACS. Approx. 300 µg of mitochondrial and nuclear extracts were mixed with Ni-NTA

beads bound to His-GST tagged OsCobB. Western blot analysis using substrate-specific primary antibody was carried out to identify the interacting proteins.

In-vivo interaction was verified by co-immunoprecipitation experiments. 5 µg of purified OsCobB antibody was incubated with protein A/G coated beads followed by incubation with 200 µL of nuclear (7.3 µg/µl) and mitochondrial (14.5 µg/µl) leaf extracts. The mixtures were centrifuged at 5000×g and the flow through was collected. Plant extracts mixed with IgG antibody was used as negative control. Finally, the beads were boiled with sample buffer and western blot analysis was performed using substrate-specific primary antibody (1:5000). Anti-OsCobB antibody was used to check for the presence of endogenous OsCobB in rice mitochondrial and nuclear leaf extracts.

4.7. *In-vitro* lysine deacylation activity assay

Steady state kinetic analysis of OsCobB deacylation was performed by keeping the fixed concentration of the nuclear/mitochondrial extract/acylated peptide and a varied concentration of NAD^+ (0–600 µM). Reaction mix containing untagged OsCobB (0.8 µM), NAD^+, substrate protein (extracted from rice leaves (20µg)) in buffer (50 mM Tris (pH 7.5), 150 mM NaCl, 5 mM DTT) was incubated at 25°C for 1-3 hr. The reaction mix was resolved in 12% SDS-PAGE and was electro-transferred on nitrocellulose membrane. Dot blot experiment was carried out using reaction mix containing acylated peptides as substrates onto a nitrocellulose membrane. The blots was blocked using 5% skimmed milk + Tris based saline (TBS) for 1 h, followed by TBST buffer wash and incubating in acylation-specific primary antibody (1:1000) for 2h. This was followed by incubation with an HRP-conjugated Goat secondary antibody (1:5000) for 45min and developed with ECL reagent (Bio-Rad) using the Bio-Rad ChemiDoc MP imaging system. The experiments were performed in triplicates. The concentration of OsCobB, NAD^+ and rice leaf extract/acylated peptide and time duration of each deacylase experiment were optimized. Protein band intensity was quantified in ImageJ. Steady state kinetic parameters were calculated using Non-Linear regression (Michaelis Menten (MM) or *kcat* Model) in GraphPad Prism version 9.1.2 (San Diego, USA).

4.8. ADP ribosylation assay of OsCobB

The ADP ribosylation reaction was performed at 25°C for 3 h. The reaction mix containing 0.8 µM recombinant OsCobB constructs, nuclear protein (20µg) in buffer (50 mM Tris pH 7.5, 150 mM NaCl, 10 mM DTT and 75 µM NAD^+ and 40 µM 6-biotin-17-NAD) was resolved in 12% SDS-PAGE followed by western blot. Rabbit monoclonal anti-biotin antibody (1:5000) was used to detect the biotinylated ADP ribose moiety of the protein.

4.9. Intrinsic tryptophan fluorescence binding assay

The assay was performed by incubating untagged OsCobB protein (0.8µM) with NAD^+ (0–200µM) at 28°C. The samples were excited at 295nm and the emission spectrum was monitored from 305 to 480 nm using Hitachi fluorimeter (Model F-4700) with a slit window of 2.5mm. The experiment was repeated with (0–500µM) H3K9Ac peptide and OsCobB (0.8µM).

4.10. *In-vitro* IDH2 enzyme assay

OsCobB (1µM) was incubated with 20µl (15.4µg/µl) mitochondrial extract (containing IDH2) for 2 h to allow the deacetylation of IDH2. The rate of NADPH released was calculated both in presence and absence of OsCobB by incubating the mix/only mitochondrial extract with 4 µM isocitrate and a gradient of $NADP^+$ (0 - 60µM) and buffer (0.2M Tris (pH-8), 10% glycerol, 1 mM $MgCl_2$) for 2 min at 25°C. Similar experiment was repeated to assess the effect of the substrate isocitrate, by incubating 20µl (15.4µg/µl) mitochondrial extract (IDH2) with 4 µM $NADP^+$ and isocitrate gradient (0 – 60 µM) in the presence as well as absence of OsCobB (1 µM) for 2 min at 25°C. NADPH released after deacetylated IDH2-catalysed reaction was monitored by measuring the absorbance at 340 nm using Shimadzu spectrophotometer. A standard curve of NADPH was prepared to calculate the rate of the IDH2 reactions. Finally, Michaelis Menten plots and the kinetic parameters were determined using GraphPad Prism 9.1.2.

4.11. *In-vitro* ACS enzyme assay

OsCobB (1µM) was incubated with 25µL mitochondrial extract (containing ACS) and 200µM NAD^+ for 1 h to allow deacetylation of ACS. The rate of NADH released was measured using an ACS activity kit both in the presence and absence of OsCobB by mixing the OsCobB-mitochondrial extract with reaction mix (50mM $MgCl_2$, 60mM NAD^+, 100mM Tris pH 7.8, 2mM CoA, 20mM ATP) and a gradient of sodium acetate (0-400mM). The reactions were incubated for 10 min at 37 °C. NADH released was measured by monitoring the absorbance at 340 nm using Shimadzu spectrophotometer. A standard curve of NADH was prepared to calculate the rate of the ACS reactions. Finally, Michaelis Menten plots and the kinetic parameters were determined using GraphPad Prism 9.1.2.

4.12. Comparison of extent of acylation with OsCobB expression during stress conditions

The amounts of the probable nuclear and mitochondrial substrates were compared in different stress conditions along with the expression level of OsCobB in the extracts. Plant growth and protein extraction was performed as indicated in 4.2 and 4.3. 30µg nuclear/mitochondrial extract of normal as well as stressed varieties of rice leaves was loaded onto a 12% SDS-PAGE and western blot analysis was done. The expression of OsCobB was determined using anti-OsCobB primary antibody. The extent of acylation was determined using anti-acyl lysine antibodies. The amounts of H3, H4, ACS and IDH2 was further determined using the protein specific primary antibody. The data was normalized using an external control (His-GST). All experiments were done in triplicates. The protein band intensities were measured using ImageJ software and bar graph was prepared by plotting the fold change in OsCobB expression in correspondence to the extent of deacylation in different stress conditions.

5. Results and Discussion

Objective 1: *In-silico* studies to understand the molecular mechanism of OsCobB

1.1. Structural characterization of OsCobB

The three-dimensional model of OsCobB was prepared using the amino acid sequence of OsCobB (Uniprot id- A2XBC4) in SWISS-model webserver (https://swissmodel.expasy.org/).

The template used for this model was *E.coli* CobB (PDB id 1S5P) having 89% sequence identity with OsCobB.

Overlaying OsCobB model with *E.coli* CobB and Human SIRT5 (PDB id 3RIY) helped in locating its substrate binding and NAD^+ binding regions. The structure of OsCobB revealed a smaller Zn^{2+}-binding and a larger Rossmann fold domain. The two domains were interlinked by numerous loops, creating a region for acylated peptide binding. The zinc ion was situated away from the active site hinting at its non-involvement in the catalytic activity of OsCobB. However, it might have a crucial role in supporting the structural stability of the catalytic core domain. Normally, 4 Cys residues are coordinately involved in formation of a tetrahedral geometry surrounding the Zn^{2+} ion[46]. But OsCobB showed a zinc binding motif of the pattern, Cys-X_2-Ser-X_{15}-Cys-X_2-Cys, where the zinc ion formed tetrahedral co-ordination with the three Cys (Cys118, Cys137 and Cys140) and another nearby Cys, Cys139. Ser did not participate in the coordination. Similar trend was observed in bacterial CobB where the Cys was replaced by Ser. The structure of OsCobB revealed various features of a SIR2-protein family, confirming that OsCobB is a sirtuin **(Fig 1)**.

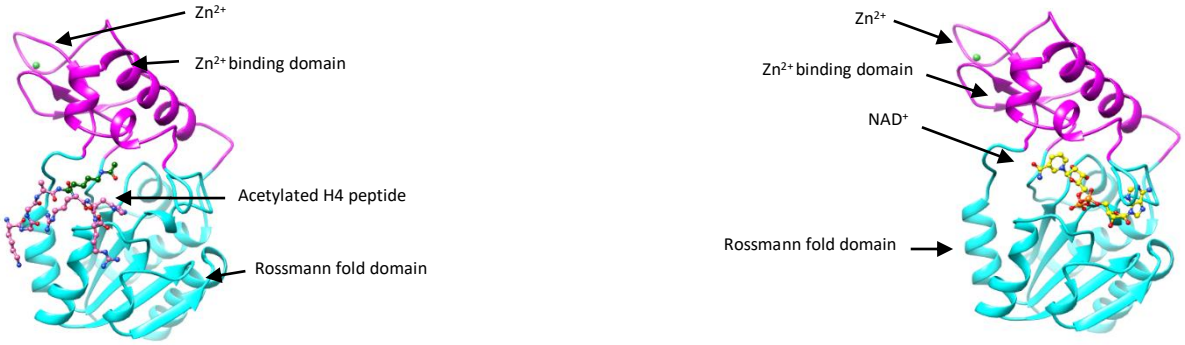

Fig 1. Structural analysis of OsCobB. Cartoon representation of OsCobB visualized in chimera 1.15. *E.coli* CobB (PBD id-1S5P) and *H.sapiens* SIRT5 (PDB id- 3RIY) were overlaid on the OsCobB model that was prepared using Swiss-model webserver to identify the binding sites for acetylated histone H4 peptide (pink ball and stick representation) and NAD^+ (yellow ball and stick representation) respectively. OsCobB shows the presence of a smaller zinc binding domain and a larger Rossmann fold domain, which establishes the protein to be a sirtuin.

1.2. Comparative phylogenetic analysis and identification of the conserved motifs required for its acylation activities

The amino acid sequence of the newly identified protein, OsCobB was compared to that of other rice sirtuins, OsSRT1 (class II sirtuin member) and OsSRT2 (class IV sirtuin member) in order to gain some hint of its sirtuin class. Multiple sequence alignment revealed that OsCobB is a small protein with no extended N- or C-terminal regions as in OsSRT1 and OsSRT2. OsCobB has 27% and 36% sequence identity with that of OsSRT1 and OsSRT2, respectively. It also possesses different substrate binding and NAD^+ binding residues when compared to OsSRT1 and OsSRT2. The CXXS motif in OsCobB, involved in Zn^{2+}-binding, is different from the other *O.sativa* sirtuins where Ser was replaced by Cys. The GXGIS**A** motif, involved in NAD^+ binding, was also observed in OsCobB, where the Ala was conserved in class III sirtuins while it was replaced by Thr in all other sirtuin classes as observed in OsSRT1 and OsSRT2. The FGE motif was also identified in OsCobB, which is another conserved motif in class III sirtuins involved in substrate binding **(Fig 2).** OsCobB showed a very low sequence identity to class II or class IV sirtuin members in comparison to class III sirtuin members, and thus it can be well placed in the category of class III sirtuins.

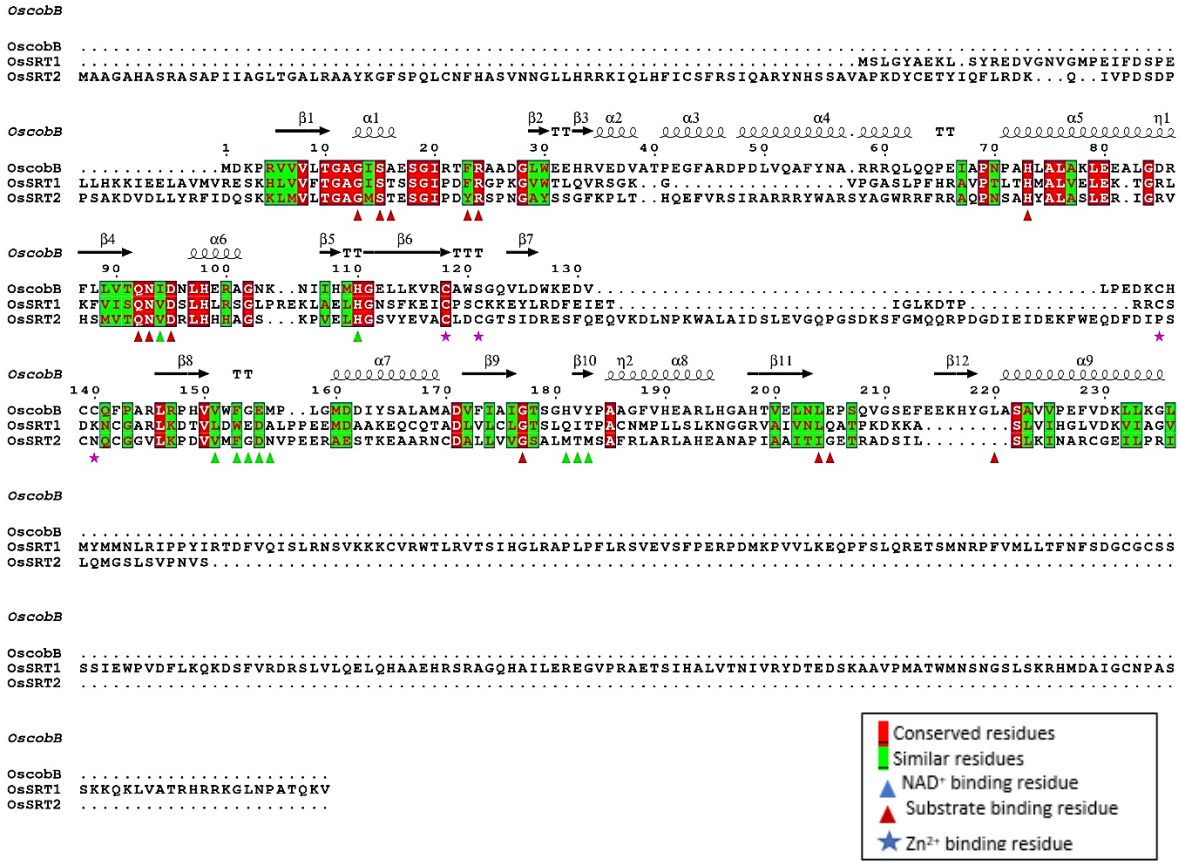

Fig 2. Sequence comparison of sirtuins of *Oryza sativa var indica*. The amino acid sequences obtained from uniprot (OsCobB- Uniprot ID A2XBC4, OsSRT1- Uniprot ID B8ARK7 and OsSRT2- Uniprot ID B8BNG4) were aligned using clustalW and visualized using ESPript 3.0. The residues involved in NAD^+-binding, substrate binding and Zinc binding are marked as blue triangles, maroon triangles and blue stars respectively. Conserved residues are highlighted in red and similar residues are highlighted in green. The depiction of α-helices and β-sheets in OsCobB structure is indicated above the sequence. Besides, the α-turn and β-turn are indicated as TTT and TT respectively. OsCobB was found to possess no extended N- or C- terminal ends and has low sequence identity with OsSRT1 (class II sirtuin member) and OsSRT2 (class IV sirtuins member). Moreover, OsCobB possessed numerous motifs conserved to class III sirtuins members.

Further sequence analysis with other class III sirtuin members revealed that OsCobB has an approx. 89% sequence identity with the bacterial sirtuin, CobB in *E.coli*, *S.typhimurium* and *S.enterica*. In comparison to that, it has a lower sequence identity (22- 36%) with human SIRT5, archeal sirtuins (Sir2Af1 and Sir2Af2) and *Plasmodium falciparum* sirtuin, PfSir2a.The CXXS motif, found in OsCobB, was conserved in all bacterial class III sirtuins while in the other members, the Ser was replaced by Cys. The 2nd pair of Cys was present as CXXC in bacterial CobB and OsCobB while in other class III members, it was available as CXXXXC motif. The GXG**I**SA motif was also conserved in OsCobB and bacterial class III sirtuins while in SIRT5 andSir2Af1, Ile was replaced by Val. The TQNID and YXXR motifs are also key features of class III sirtuins with exceptions to archeal sirtuins and PfSir2a **(Fig 3a).** This motif is involved in lysine desuccinylation and demalonylation[8,28] and was seen to be present in OsCobB, predicting the protein to accommodate the negatively charged groups at their active site. Phylogenetic analysis of class III sirtuins using MEGA software has grouped them into three main branches. PfSir2a was most distant from all other class III sirtuins, acting as outgroup. SIRT5 was found to be distant from both archeal as well as bacterial sirtuins and can be grouped as a separate subclass. OsCobB had the closest homology to the bacterial members and can be grouped in the same subclass **(Fig 3b)**. Hence, it can be said that OsCobB is evolutionarily closer to bacterial sirtuins. Since the differences in protein sequence often dictate the substrate specificity, it would be interesting to relate it with the functions of OsCobB.

a)

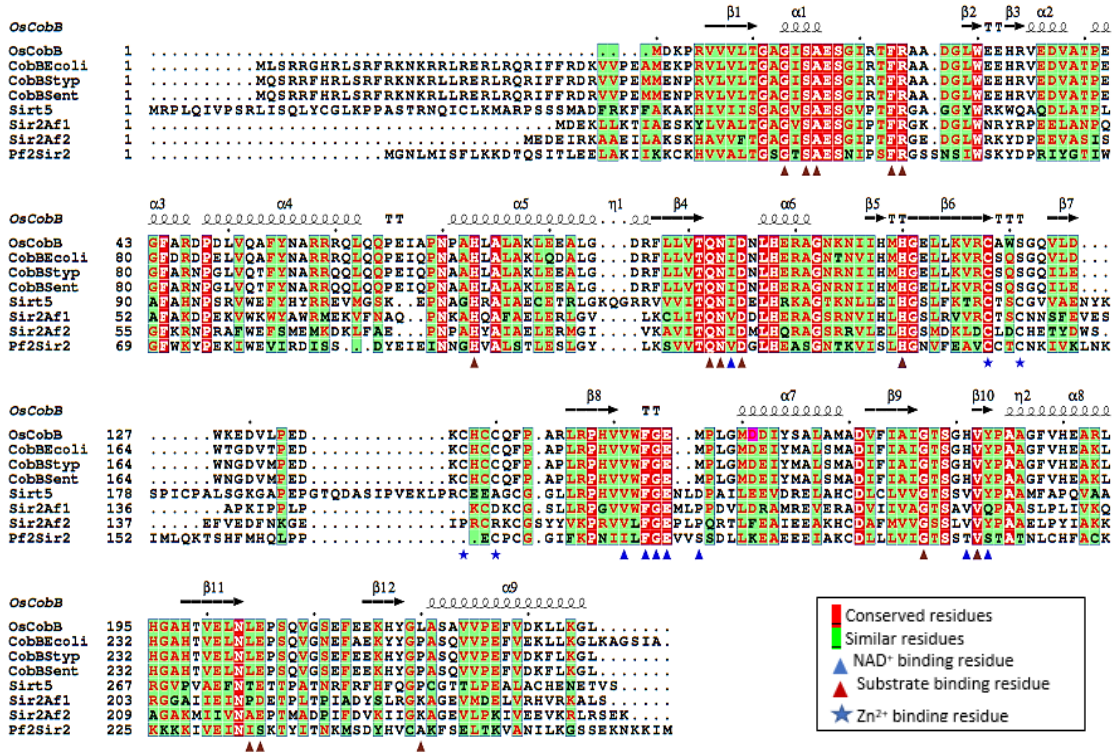

b)

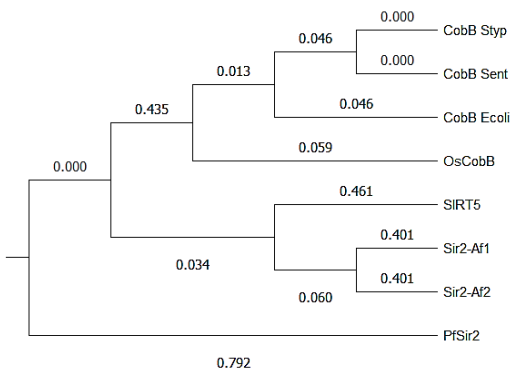

Fig 3. Comparative analysis of class III members of the sirtuin family. a) Multiple Sequence alignment of class III sirtuin members against OsCobB. The amino acid sequences of the sirtuins (NP_415638.3- CobB *E.coli*, NP_460191.1- CobB *Salmonella enterica*, WFG56040.1- CobB *S.typhimurium*, XP_024302154.1- SIRT5 *Homo sapiens*, O28597.1- Sir2-Af1 *Archaeoglobus fulgidus*, O30124.1- Sir-Af2 *A. fulgidus* and Q8IE47.1- PfSir2 *Plasmodium falciparum*) were taken from NCBI and aligned using clustalW and visualized using ESPript 3.0. The residues involved in NAD^+-binding, substrate binding and Zinc binding are marked as blue triangles, maroon triangles and blue stars respectively. Conserved residues are highlighted in red and similar residues are highlighted in green. The depiction of α-helices and β-sheets in OsCobB structure is indicated above the sequence. Additionally, the α-turn and β-turn are indicated as TTT and TT respectively. b) Comparative phylogenetic analysis of class III sirtuin members. The aligned amino acid sequences were used to create the rooted phylogram using Mega X 11.0.11 software by maximum likelihood (ML) analysis showing the closeness of OsCobB to bacterial class III members rather than the eukaryotic and archeal members of the class. The branch lengths indicate the number of substitutions per site. The substitution

model is based on Jones-Taylor-Thornton (JTT) amino acid substitution model with phylogenetic test based on Bootstrap method (no. of bootstrap replications= 1000).

1.3. Molecular simulation and docking studies to determine the possible bioactive conformations of its substrates

Since OsCobB catalyzed the bi-substrate reaction (acetylated protein and NAD^+), the order of their binding needed to be determined to understand the molecular mechanism of the enzyme. Intrinsic tryptophan fluorescence assay revealed a strong binding of NAD^+ to OsCobB, indicated by the lowering of fluorescence intensity at 340nm on excitation of sample at 295 nm **(Fig 4a.i)**. In comparison, mixing of OsCobB with acetylated H3K9 peptide did not lower the fluorescence intensity effectively, even at the concentration of 500 µM **(Fig 4a.ii).** However, further lowering of fluorescence intensity was observed when 10 µM NAD^+ was added to the same mix. This indicated that binding of the NAD^+ may result in conformational changes at the active site facilitating the proper binding of the peptide **(Fig 4a.iii).**

This analysis was further supported by molecular dynamics simulation studies. The apoenzyme form of OsCobB demonstrated an exposed substrate and NAD^+-binding regions even after 200 ns **(Fig 4b.i).** But binding of NAD^+ led to the formation of a closed conformation at the NAD^+-binding site, further forming a hydrophobic tunnel at the peptide binding site **(Fig 4b.ii).** Although, binding of H3K9ac peptide alone did not lead to the formation of any hydrophobic tunnel at the substrate binding site. Furthermore, the peptide was loosely bound to the OsCobB surface **(Fig 4b.iii).** Conversely, binding of both the H3K9ac peptide and NAD^+ was observed to bring about a modification at the peptide binding site to form a hydrophobic cavity **(Fig 4b.iv).** The formation of the hydrophobic cavity involved a bridge formation between Trp152, Phe153 and Val182 **(Fig 4c).** V151 was also involved in hydrogen bond formation with N€ of acetyl lysine, which was essential for deacetylation activity of OsCobB. Hence, binding of NAD^+ was deduced to be essential for effective incorporation of the substrate in case of OsCobB.

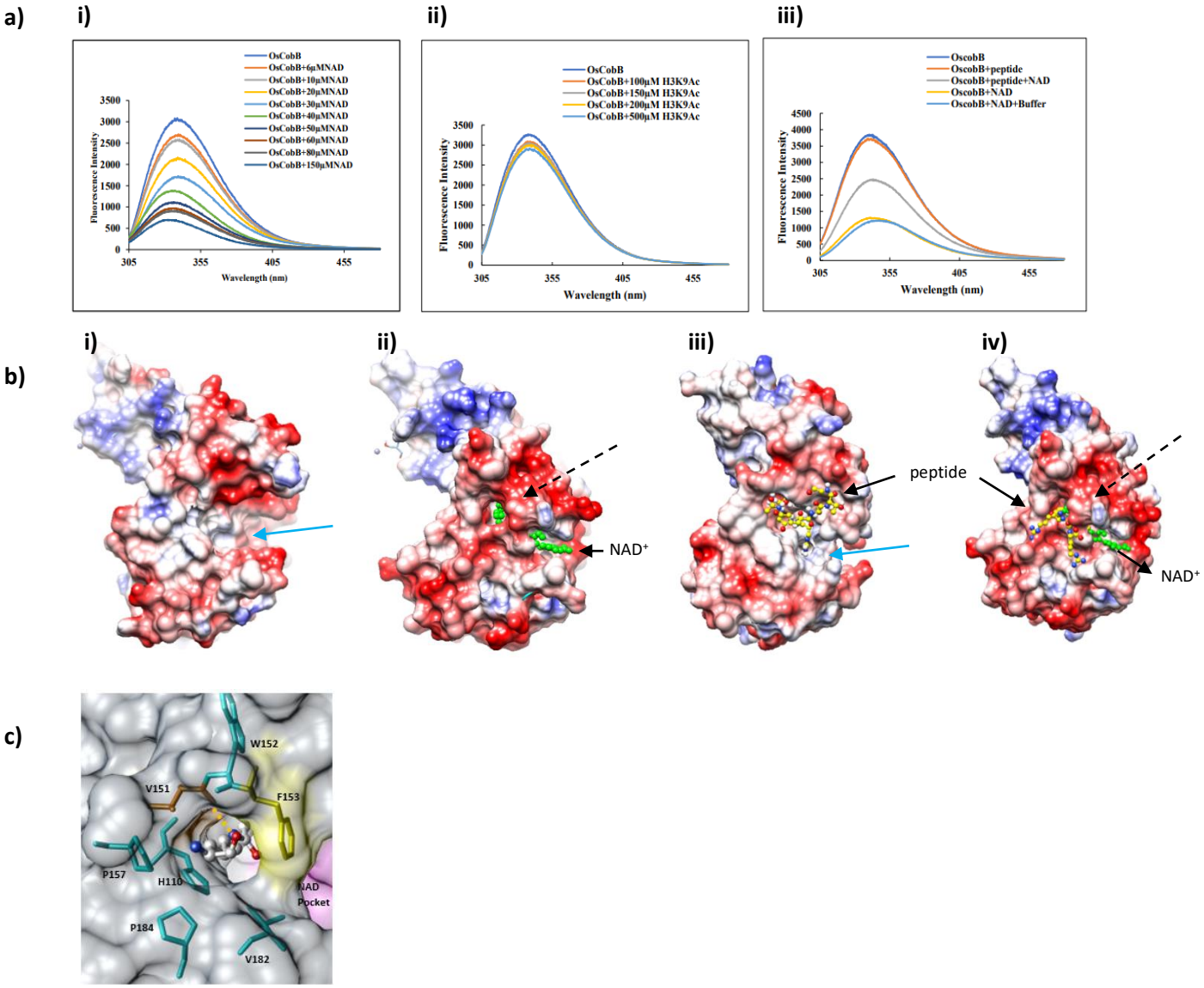

Fig 4. Binding of the substrate and the cofactor to OsCobB leading to structural modifications. a) Intrinsic tryptophan fluorescence spectra of untagged OsCobB highlighting the decrease in fluorescence intensity due to the addition of (i) NAD^+ (0-100μM), (ii) H3K9Ac peptide (0-500μM), and (iii) NAD^+ (100 μM) and H3K9Ac peptide (0-500μM). There was a significant drop in fluorescence intensity when NAD^+ was added to the peptide, which otherwise, showed the least drop in intensity. b) Molecular simulation studies to understand the structural modifications as a result of binding of (i) apoenzyme, (ii) NAD^+, (iii) H3K9ac peptide and (iv) both NAD^+ and H3K9ac peptide. The figures are based on analysis using GROMACS and the figures are prepared in UCSF Chimera. NAD^+ shown in green sphere representation and H3K9ac peptide shown in yellow heteroatom ball and stick representation. Charged surface representation of OsCobB displaying electrostatic potential in a colour gradient between red (-10KB_T/e) and blue (+10KB_T/e), white colour denoting neutral. The apoenzyme and OsCobB-H3K9 peptide bound structures revealed an open conformation at the active site (shown by blue pointed arrow). The peptide binds loosely at the peptide binding site in case of the OsCobB-peptide bound structure. In the NAD^+ bound structures, there was a cleft formation at the peptide binding site (shown as black dotted arrow) which, in turn, resulted in proper binding of the peptide to OsCobB. c) The

incorporation of acetylated H3K9 ligand, displayed in grey as heteroatoms in ball and stick representation. The figure highlights the important hydrophobic residues that are involved in peptide binding. V151 forms a H-bond with the modified lysine residue and is involved in catalysis.

To get an idea about the other deacylase activities in OsCobB, molecular docking was carried out with peptide containing acylated lysine modifications using autodock vina. All modifications were found to be accommodated into the peptide binding cavity of OsCobB. The13-carbon long side chain of the myristoyl peptide initially faced hindrance at the peptide binding site **(Fig 5a)**.The length of the peptide binding cavity was measured to be 9.64Å, which is shorter than the length of the myristoyl modification (20.07Å). Sir2Af2,another class III sirtuin, has been reported to undergo a conformational change in order to accommodate the myristoyl modification[47]. So it may be possible that OsCobB also needs to undergo some structural modification to accommodate such long chain acyl groups. Preparing a model structure of OsCobB taking Sir2Af2-Myristoyl peptide bound structure (PDB id 4TWJ) in Swissmodel, followed by docking analysis, could accommodate the long chain, though the binding energy remained very low **(Fig 5b)**. The H3K9 peptides with acetyl, succinyl, malonyl and ß-hydroxybutryl modifications were seen to have the strongest binding though the total number of bonded and non-bonded interactions was highest for glutaryl, HIB and BHB lysine peptides **(Table 1).** 2-D representation of OsCobB-acyl modifications showed the importance of Tyr55 and Arg58 in strongly binding of the side chains at the catalytic site. BeatMuSiC v1.0 online software was used to mutate the probable substrate binding residues which showed a significant drop in the binding affinity of the peptides **(Fig 5c)**. V151, W152, F153, G154 and H110 mutations were documented to decrease the binding affinity of H3K9 acetyl, succinyl and malonyl peptides. The Y55G and R58A mutations also resulted in the drop in binding affinity in malonyl, glutaryl and succinyl peptides. Since no information is available about class III sirtuin in plants, it would be interesting to determine the possible enzyme activities of OsCobB *in-vitro* and *in-vivo.*

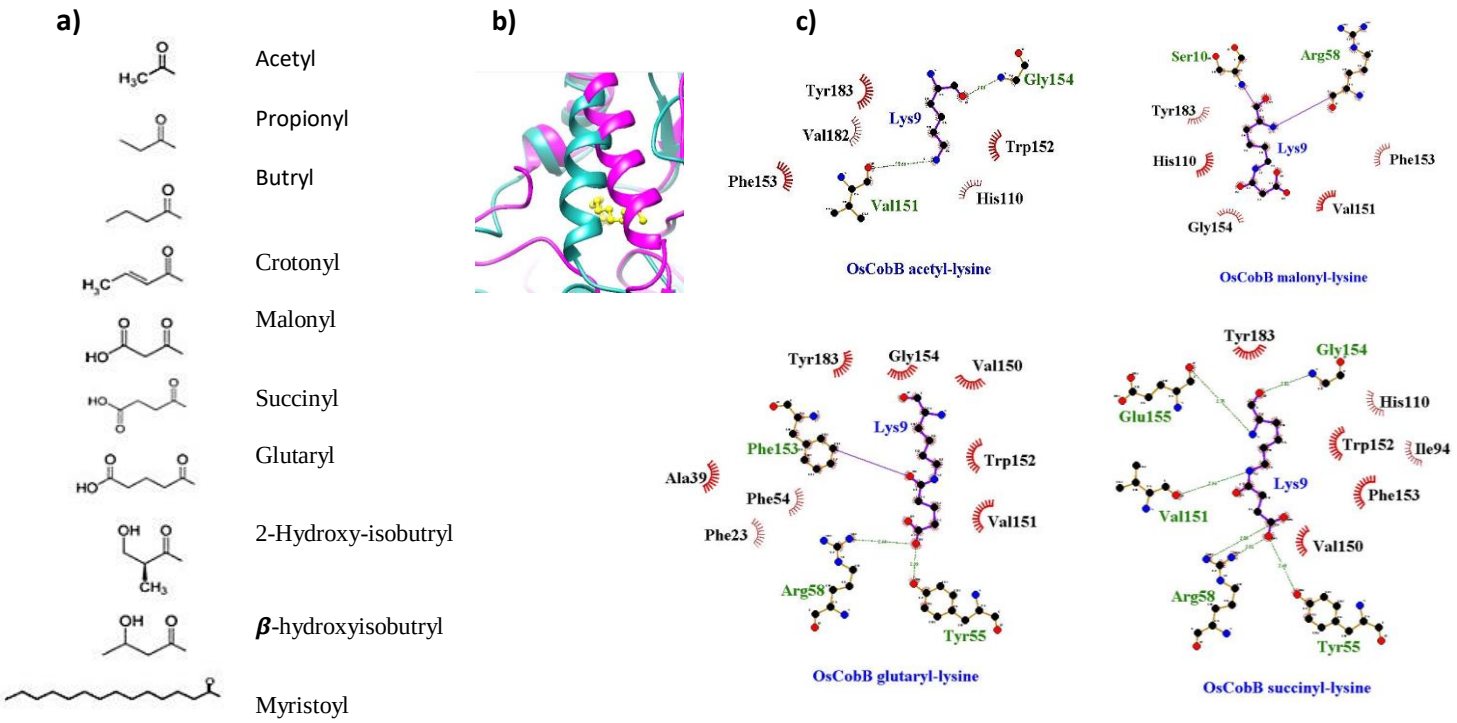

Modification	$\Delta\Delta G_{Bind}$ (kcal/mol)				
	Y55- G	R58- A	V151- K	F153- G	W152- E
Acetyl	0.03	0.02	-1.52	-2.35	-1.51
Malonyl	-1.66	-0.60	-2.07	-2.80	-2.35
Succinyl	-1.76	-0.59	-2.07	-2.41	-1.91
Glutaryl	-1.66	-0.60	-1.06	-1.20	-1.71

Fig 5. Incorporation of different acylation modifications at the substrate-binding site of OsCobB. a) Chemical structures of different acyl modifications showing the differences in their side chains. b) Ribbon representation of OsCobB apoenzyme (in magenta ribbons) overlayed with the protein docked with myristoylated (yellow ball and stick representation) H3K9 peptide (in cyan ribbons). Both the protein models have been prepared using Swiss-model webserver and visualized using UCSF Chimera. OsCobB probably needs to undergo a conformational change involving the shift of the α-helix in order to accommodate the long length of the modification. c) 2 dimensional schematic diagrams of OsCobB docked with the acylated K9 residue of histone H3 using Autodock vina and visualized using Ligplot^{+} v2.2. The hydrogen bonds are indicated by green dotted lines and the hydrophobic interactions are indicated by red arc-like representation with spookes. Tyr55 and Arg58 residues of OsCobB formed hydrogen bonds with the carboxyl oxygen atom in malonyl, succinyl and glutaryl peptides. Table shows the prediction of the

alterations in protein-peptide binding energies on mutation performed in beatMuSiC v1.0 online software. OsCobB protein was mutated at various residues predicted to be involved in substrate binding in relation to H3K9ac, H3K9succ, H3K9mal and H3K9glu peptides. $\Delta\Delta G_{bind}$ in red denotes the net reduction in binding energy resulting from each mutation. A decrease in binding affinity demonstrateS the involvement of residues like F153, W152, G154, H110 and V151 in peptide binding. Y55 and R58 mutations also decreased the binding affinity in malonyl, succinyl and glutaryl peptides as they are directly involved in binding to the modification.

Acyl modifications of histone H3K9 peptide	Binding score (Kjoules/mol)	No of Hydrogen bonds	No of non-bonded interactions
Acetyl	-26.7776	3	40
Propionyl	-19.6648	2	47
Butryl	-26.7776	3	40
Crotonyl	-24.2672	2	89
Malonyl	-32.2168	2	92
Succinyl	-31.38	5	87
Glutaryl	-28.451	4	146
HIB	-18.828	4	112
BHB	-34.7272	8	163
myristoyl	-3.765	5	13

Table1 - Prediction of preferred acyl modification for binding at the active site. Prediction of binding affinity based on docking score and the number of hydrogen and non-bonded interactions between the acyl modification and OsCobB. Though the binding energy was found to be highest in acetyl, succinyl, malonyl and ß-hydroxybutryl modifications of the H3K9 peptide, the number of interactions were highest in glutaryl, HIB and BHB lysine peptides.

Objective 2- Determination of the possible enzyme activity and its regulation in plants

2.1. Identification of its subcellular localization

Whole protein was extracted from different tissues of IR64 variety of rice plant and western blot analysis was done using OsCobB-specific primary antibody which revealed that OsCobB is mostly localized in the leaf, sheath, flag leaf and stem tissues while a low concentration of the protein is present in roots and panicle. No OsCobB protein was detected at the seedling stage **(Fig 6a).** Further, OsCobB was revealed to be mostly localized in the mitochondria with trace amounts in the nucleus (21%) as well **(Fig b).** The purity of the mitochondrial and nuclear

fractions was confirmed using compartment specific markers. Mitofate, RSLpred as well as TargetP 2.0 localization prediction softwares also implied on its mitochondrial localization[48–50]. This is the first plant class III sirtuin to show dual localization. When compared to the other rice nuclear sirtuin, OsSRT1 and mitochondrial sirtuin, OsSRT2, it would be intriguing to discover the need of another sirtuin in rice. We may further speculate that OsCobB might have the ability to translocate between the two organelles during specific stress conditions in order to regulate the specific pathways involved in stress management. Literature studies have proclaimed that sirtuins like SIRT3 and SIRT5 can translocate between organelles upon cellular stress[51,52]. It is possible that this translocation activates the regulation of various stress response mechanisms in plants.

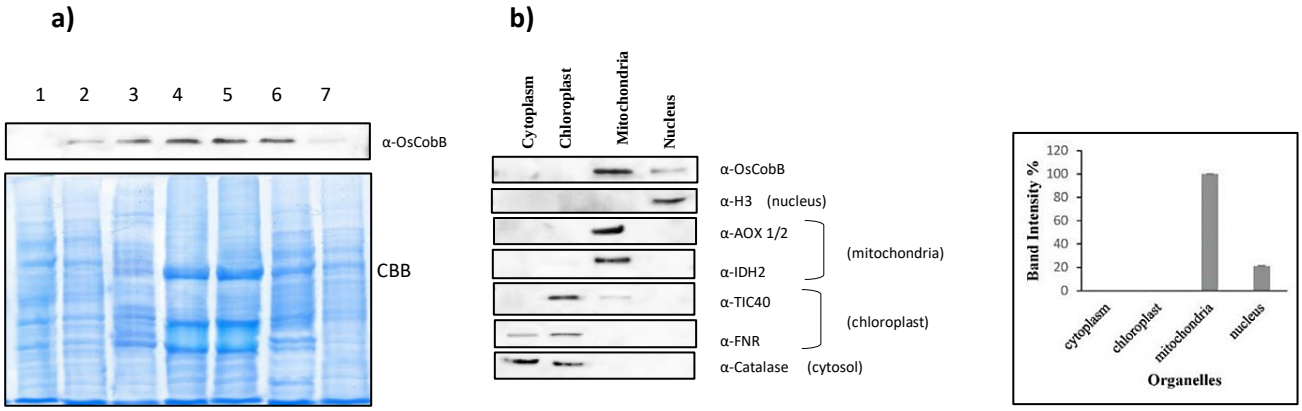

Fig 6. Localization of OsCobB protein. a) Tissue localization of OsCobB. 7ug of protein extracted from various plant parts were loaded on 12% SDS-PAGE and confirmed by western blot analysis using OsCobB-specific primary antibody. Extracts that were taken into consideration are Lanes 1- Seedling, 2- root, 3- stem, 4- leaf, 5- sheath, 6-flag leaf, 7- panicle. OsCobB protein was dominant in the stem, leaf, sheath and flag leaf extract. However, traces of the protein were seen in root and panicle extracts. The seedling extract was devoid of OsCobB protein. b) Distribution of subcellular OsCobB expression in unstressed leaf. Lane 1- cytosolic extract, lane 2- chloroplast extract, lane 3- mitochondrial extract, lane 4- nuclear extract. OsCobB antibody was used to detect the expression of the endogenous protein in those samples. The different plant extracts were verified using specific marker antibodies. OsCobB was majorly localized in mitochondria while an appreciable amount was found in the nucleus as well. The bar graph shows OsCobB expression to different subcellular organelles. The bar graph portrays the amount of OsCobB based on the band intensities in western blot, calculated by ImageJ software.

2.2 *In-vitro* OsCobB- catalyzed deacylation studies and comparative analysis of its kinetic parameters among members of class III sirtuins

2.2.1 Search for nuclear substrates of OsCobB

As sirtuins are histone deacylases, OsCobB was examined for its histone interacting partners owing to its nuclear localization. Nickel pull down assay using His GST-tagged OsCobB and untagged histones revealed that OsCobB binds to histones H3 and H4 but not to H2A, H2B or H1 histones **(Fig 7a).** Co-immunoprecipitation assays with OsCobB also confirmed the *in-vivo* interaction with histones H3 and H4 **(Fig 7b).** *In-vitro* deacetylation assay was performed at different time points (0- 105 min) using histone H3 from leaf nuclear extract to detect positive deacetylase activity of the protein **(Fig 7c)**.Further, OsCobB was able to deacetylate histone H3 at lysine residues K9 and K18 but not at K14, K27 or K56 residues **(Fig 7d).**The K_M for NAD^+ was calculated to be 135.5 ± 12µM and 104 ± 16µM for H3K9ac and H3K18ac residues respectively. Furthermore, OsCobB could deacetylate H3K9ac (k_{cat}/K_M as 369 $M^{-1}s^{-1}$) more efficiently than H3K18ac (k_{cat}/K_M as 176 $M^{-1}s^{-1}$), as indicated by its higher k_{cat}/K_M value. Molecular docking of OsCobB with H3K9ac and H3K18ac peptides revealed that the H3K18ac peptide penetrated deeper into the peptide binding cavity in comparison to H3K9ac peptide. However, there was a hydrogen bond formation between Val151of OsCobB and N-€ amino group of the H3K9ac peptide along with Thr22 of OsCobB, which forms H-bond with the N-***α*** amino group in H3K9ac peptide. On the other hand, Val151 is involved in hydrophobic interaction in case of H3K18ac peptide. This may lead to stronger enzyme efficiency towards H3K9ac peptide **(Fig 7e).**

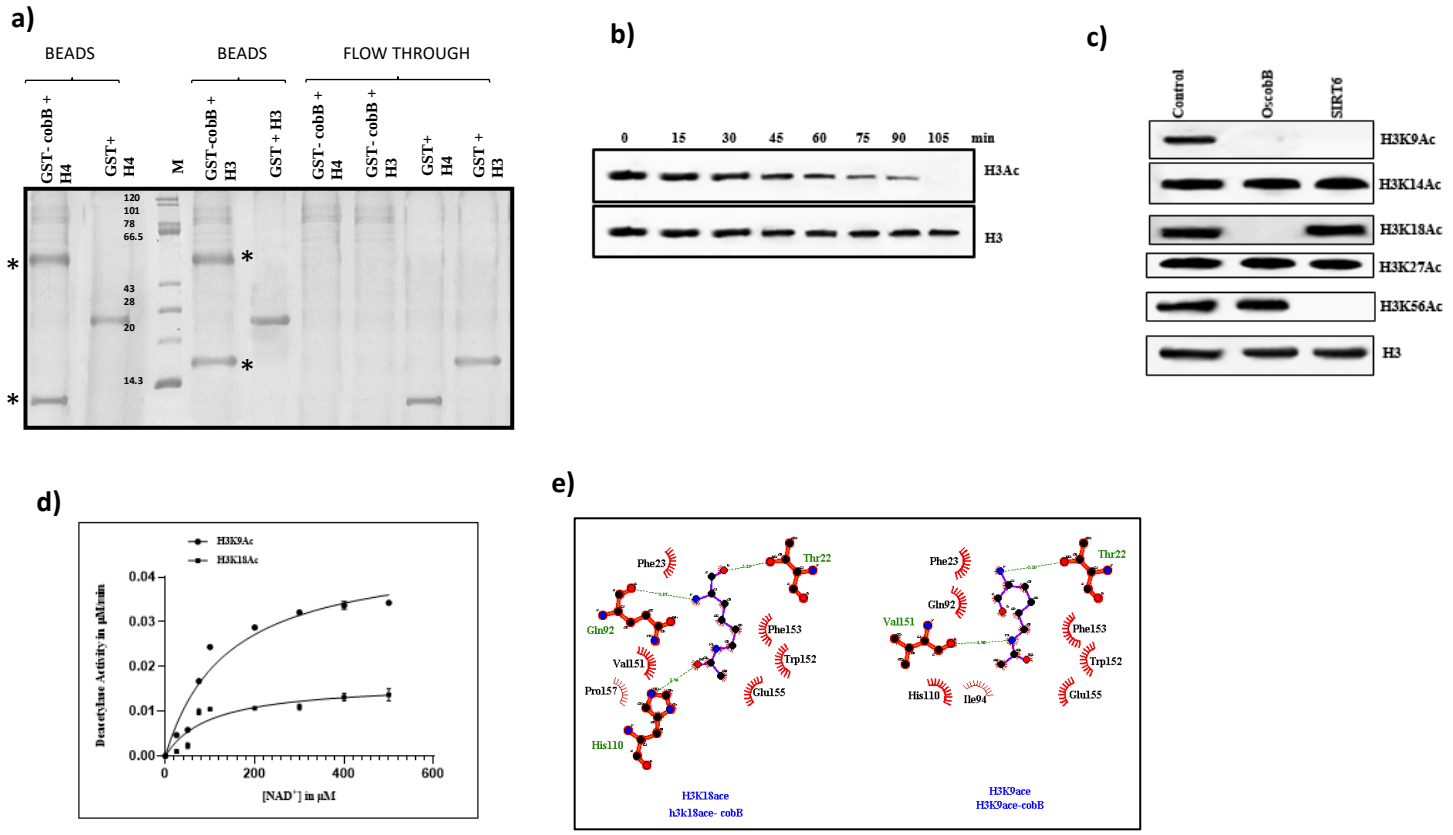

Fig.7. Detection of histone targets for OsCobB catalyzed acetylation processa) A coomassie blue stained 12% (w/v) SDS/PAGE gel showing binding of GST-tagged OsCobB protein (54.5kDa) with recombinant histones H3 (17kDa) (lane 4) and H4 (13.7kDa) (lane 1) on Ni-NTA agarose beads after Ni- pull down assay. GST protein alone was interacted with the histones as a negative control in lanes 2 and 6 which show no histone bands indicating that there is no non-specific binding of the histones to GST or Ni-beads. The asterisks point out the interacting partners. b) Western blot analysis showing *in-vitro* deacetylation of histone H3 from leaf nuclear extract over a time period of 0 to 105 min. The enzymatic reactions were stopped by adding sample buffer and boiling the mix at 95 °C. Western blot analysis was performed using acetyl H3 primary antibody to check the deacetylation ability of OsCobB. Loading control was analyzed using–histone H3 primary antibody. c) Western blot analysis using antibodies specific for certain histone H3 lysine sites to detect the site specific deacetylation abilities of OscobB. Lanes 1- empty pET28a vector used as negative control, 2- recombinant OsCobB, 3- purified Human SIRT6 used as negative control. Anti- histone H3 primary antibody was used as loading control for the western blot analysis. d) Michaelis-Menten plot comparing the kinetic parameters for NAD^+ in the deacetylation of H3K9ac and H3K18ac from leaf nuclear extract of unstressed rice variety. A gradient of NAD^+ (0-600 µM) was used. Plot was done in non-linear regression model using GraphPad prism 8.3.0. e) Docking analysis of OsCobB with peptides, H3K9ac and H3K18ac, visualized in Ligplot$^+$. The figures show H-bond formation between the H3K9 acetyl modification and V151. H110 forms H-bond in case of H3K18ac while it is involved in hydrophobic bond formation in H3K9ac. There are a number of other hydrophobic residues involved- F23, I94, and T22 which are involved in the formation of hydrophobic cavity at the peptide binding site.

In-vitro deacylation assay was performed using different acyl modifications of histone H3K9 peptide. Comparing it with molecular docking studies revealed that OsCobB could accommodate different acyl modifications effectively at the peptide binding site with varying binding energies. OsCobB was seen to have highest enzymatic efficiency for glutaryl modifications, followed by acetyl, succinyl and malonyl modifications **(Table 2).** It could deacylate all peptides having the weakest efficiency for the myristoylated peptide. This data was in sync with the molecular docking analysis which revealed the presence of a stronger interaction between the succinyl, malonyl and glutaryl side chains and Tyr-55 and Arg-58 residues of OsCobB **(Fig 8).** The succinyl peptide can penetrate deeper into the acyl-lysine cavity with a specific recognition of negatively charged acyl groups by OsCobB. A similar trend was observed in human SIRT5 also has an inclination towards desuccinylation and demalonylation of its substrates, GDH K503, ACS K628 and H3K9 rather than deacetylation[12]. It can also be noted that OsCobB was most efficient in deglutarylation and demalonylation of histone H3 *in-vivo*, along with deacetylation and desuccinylation of histone H3 extracted from rice leaves **(Table 3).** Comparing the kinetic parameters to SIRT5, it was found to be synchronous with the human sirtuin **(Table 4)**. It had been previously reported that SIRT5 could demalonylate and desuccinylate H3K9 with a very high efficiency (k_{cat}/K_m 6100 $M^{-1}s^{-1}$ and 4300 $M^{-1}s^{-1}$, respectively)[12].These similarities in their enzymatic preferences further prove the classification of OsCobB as a class III sirtuin member.

H3K9 acyl peptide modifications	***Km* for NAD^+ (μM)**	***kcat* (min^{-1})**	***kcat/Km* ($M^{-1}s^{-1}$)**
Acetyl	139 ± 12	3 ± 0.1	360.432
Propionyl	197 ± 95	2.6 ± 0.02	220.40
Butryl	115 ± 12	1.13 ± 0.1	164.096
Crotonyl	231 ± 22	3.5 ± 0.002	253.03
Malonyl	183.4 ± 15.5	1.17 ± 0.1	106.53
Succinyl	185.3 ± 20.8	1.863 ± 0.001	167.90
Glutaryl	244 ± 96	6.5 ± 0.02	444.877
2-hydroxy isobutryl	368 ± 73	1.2 ± 0.002	54.457

Myristoyl	ND	ND	ND

Table 2- A comparison of the kinetic parameters for NAD^+ in OsCobB catalyzed deacylation of histone H3K9 peptide. Reactions were carried out with 0-800 µM NAD^+ with constant concentration of H3K9 acyl peptides (1µg). Dot blot technique was adopted using acyl-specific primary antibody in order to calculate the degree of acylation. ND means not determined. The K_M for the same could not be calculated as the enzyme was unable to reach its saturation even after 2 hours of reaction time. On the other hand, this table pinpoints at the efficient desuccinylase and demalonylase activity of OsCobB in comparison to the other modifications.

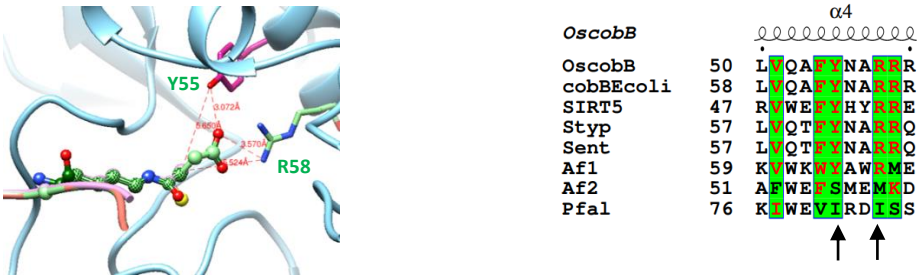

Fig 8. Molecular docking analysis in support of desuccinylation and demalonylation activity of OsCobB. Three-dimensional ribbon representation of OsCobB bound to H3K9 succinyl (light green ball and stick representation) and malonyl (dark green ball and stick representation) peptides by docking using Autodock Vina and visualized in chimera 1.15. It is seen to form a bond with Y55 and R58, indicating that OsCobB may be involved in desuccinylation and demalonylation of its substrates.

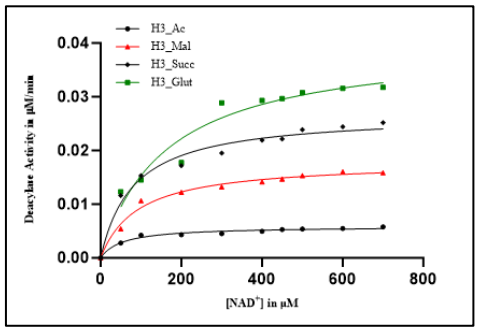

Kinetic Parameters	H3 acetyl protein	H3 succinyl protein	H3 malonyl Protein	H3 glutaryl protein
K_{cat} (min^{-1})	0.3911 ± 0.013	1.8 ± 0.07	1.2 ± 0.04	2.7 ± 0.2
K_m (µM)	54.44 ± 10.3	81.5 ± 14	92.11 ± 13	244 ± 88
K_{cat}/K_m ($M^{-1}s^{-1}$)	120	368	217	278

Table 3- Comparison of the kinetic parameters for NAD^+ in OsCobB catalyzed H3 deacylation. Kinetic parameters for OscobB deacylase activity of histone H3 protein extracted from rice leaves was measured after western blot analysis. Reactions were carried out with 0-800 µM NAD^+ with constant concentration of nuclear extract containing histone H3 (20µg). This table pinpoints at the efficient deacylase activities of OsCobB in comparison to the other modifications.

Protein	K_M(µM)	k_{cat} (s^{-1})	k_{cat}/K_M($M^{-1}s^{-1}$)	Substrate	Activities mentioned
Sir2Af2	84 ± 22	0.220	2619	p53	Deacetylation [53]
Sir2Af1	387 ± 99	0.136	351	p53	Deacetylation [53]
Sir2Af1	2.12 ± 0.35	0.235 ± 0.027	110849	BSA	Deacetylation[54]
PfSir2A	39 ± 9	0.001 ± 0.0002	26	H3K9	Deacetylation[13]
PfSir2A	8 ± 1	0.001 ± 0.0002	125	H3K9	Debutyrylation[13]
PfSir2A	1.2 ± 0. 3	0.001 ± 0.004	833	H3K9	Deoctanylation[13]
PfSir2A	<1	0.01 ± 0.002	ND	H3K9	Demyristoylation[13]
CobB Ecoli	15.1 ± 0. 50	0.135 ± 0.007	8940	H3K9	Deacetylation[5]
CobB Ecoli	86 ± 11	0.242 ± 0.040	2813	H3K9	Desuccinylation[5]
SIRT5	>750	ND	7.8	H3K9	Deacetylation[12]
SIRT5	6.1 ± 2.8	0.037 ± 0.003	6100	H3K9	Demalonylation[12]
SIRT5	5.8 ± 2.7	0.025 ± 0.002	4300	H3K9	Desuccinylation[12]
SIRT5	>750	ND	<2	GDH K503	Deacetylation[12]
SIRT5	8.7 ± 1.3	0.014 ± 0.001	1600	GDH K503	Demalonylation[12]
SIRT5	14 ± 4	0.028 ± 0.002	2000	GDH K503	Desuccinylation[12]
SIRT5	>750	ND	18	ACS2 K628	Deacetylation[12]
SIRT5	150 ± 40	0.079 ± 0.008	5200	ACS2 K628	Demalonylation[12]
SIRT5	450 ± 150	0.268 ± 0.051	60	ACS2 K628	Desuccinylation[12]

Protein	K_M(µM)	Substrate	Activities mentioned
SIRT5	459.6 ± 86	HMGCS2	Desuccinylation[55]
Protein	**K_d(mM)**	**Substrate**	**Activities mentioned**
SIRT5	0.92 ± 0.23	NAD^+	Deacetylation[56]

Table 4- A collection of kinetic parameters among members of class III sirtuins. Reported catalytic efficiencies of all class III members along with their target deacylase activities were accumulated in order to compare the enzymatic capability of OsCobB with the other class III sirtuins members. It would also give an idea about the regulation of the deacylase activities. ND= Not determinable.

On the other hand, OsCobB could not deacetylate histone H4 at lysine residues K5, K8, K12, K16 and K20 **(Fig 9a).** So it would be interesting to find the other deacylation activities that it

may possess. Time dependent deacylation assay (0-240 min) using histone H4 extracted from rice leaves and comparing the extent of acylation brought to light the preferential deacylation of OsCobB in association to histone H4. It was discovered that OsCobB has no prominent demyristoylation of histone H4 by OsCobB even after 240 min, presumably due to the requirement of conformational changes in OsCobB for the incorporation of the modification. Glutarylation, butrylation, propionylation and crotonylation were the most favourable targets in case of histone H4 **(Fig 9b).** *In-vivo* deacylation assay using histone H4 extracted from rice leaves also showed the dominance of OsCobB deglutarylase activity (k_{cat}/k_m 729 $M^{-1}s^{-1}$) **(Fig 9c).** H4 desuccinylation and demalonylation were also preferred to deacetylation as catalytic targets.

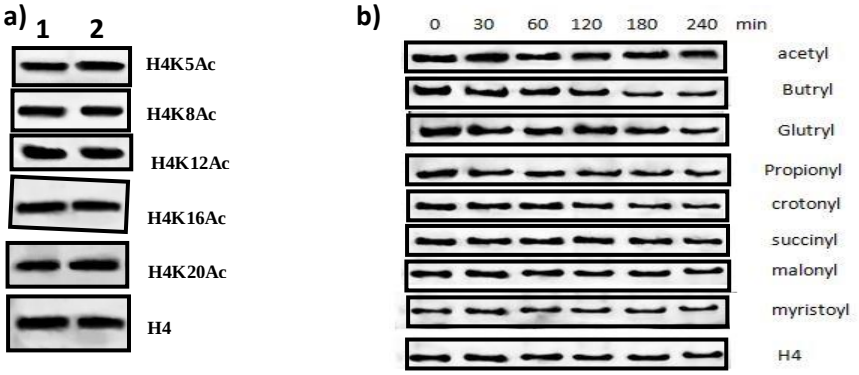

c)

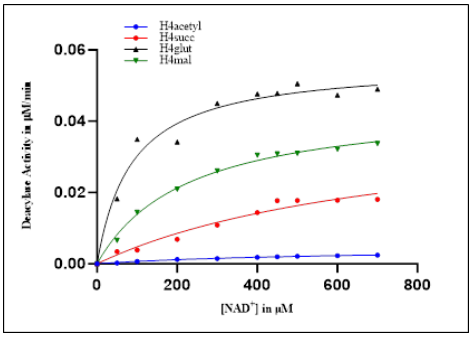

Kinetic Parameters	H4 acetyl protein	H4 succinyl protein	H4 malonyl Protein	H4 glutaryl protein
K_{cat} (min^{-1})	1.3 ± 0.1	2.7 ± 0.74	3 ± 0.2	3.75 ± 0.0.2
K_m (µM)	569 ± 74	771 ± 333	227 ± 38	86 ± 18
K_{cat}/K_m ($M^{-1}s^{-1}$)	38	65	222	729

Fig.9- Detection of the preferred deacylation activity of histone H4 for OsCobB. a) Western blot analysis using antibodies specific for some histone H4 lysine sites using leaf nuclear extract from unstressed rice variety to detect the site specific deacetylation abilities of OsCobB. Lanes 1- recombinant OsCobB, Lane 2- empty pET28a vector used as negative control for the deacetylation reaction. Anti- histone H4 primary antibody was used as loading control for the western blot analysis. OsCobB did not deacetylate at K5, K8, K12, K16 or K20 residues. b) Western blot analysis displaying *in-vitro* deacylation of histone H4 from leaf nuclear extract over a time period of 0 to 240 mins. The catalytic reactions were halted by adding sample dye and boiling the mixture at 95 °C. This was followed by western blot analysis using acylation specific primary antibody for the detection of extent of deacylation. Measuring and comparing the band intensities using ImageJ showed the maximum difference in glutaryl, butryl,

propionyl and crotonyl side chains in comparison to the other modifications. c) Steady state enzyme kinetics involving acylated histone H4 protein. K_m and V_{max} values were calculated for the utilization of NAD^+ in deacylation of the H4 protein from nuclear extract. OsCobB seems to deglutarylate histone H4 most efficiently.

Beside histones, co-immunoprecipitation assay has revealed the interaction of OsCobB with nuclear Acetyl-CoA Synthetase (ACS) (OsI_07465) **(Fig 10.a).** The interacting partner was identified using ACS specific primary antibody. Nuclear ACS in humans (uniprot id Q9NUB1) display cytoplasmic localization that was seen to undergo phosphorylation at Ser659 to expose the nuclear localization signal for its movement into the nucleus[58]. ACS was found to be deacetylated by SIRT1 at Lys661 (homologous to Lys667 in rice) in mammalian cells[59]. OsCobB was also seen to deacetylate as well as desuccinylate endogenous ACS. Comparing the kinetic parameters indicated that OsCobB had a preference towards desuccinylation of ACS (k_{cat}/K_m ACS_{succ} 1199 $M^{-1}s^{-1}$) **(Fig 10.b).**

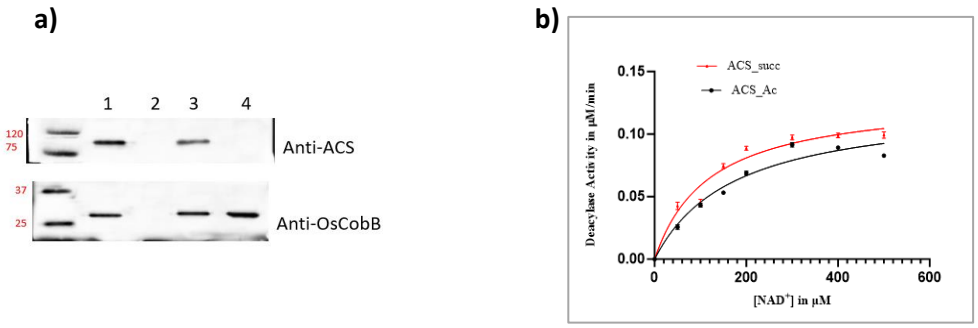

Substrate proteins	K_m for NAD^+ (µM)	k_{cat} (min^{-1})	k_{cat}/K_m (M^{-1} s^{-1})
ACSac	173.6	8.310	797
ACSsucc	119.7	8.632	1199

Fig 10. Non-histone target substrate for OsCobB. a) Co-immunoprecipitation assay showing the *in-vivo* interaction between OscobB and nuclear ACS. 5µg of purified OscobB antibody was incubated with protein A/G beads followed by incubation with 1 mg nuclear extract (lane 1). 5ug of IgG antibody was used as negative control (lane 2). Lane 3 and 4 are nuclear extract and recombinant OsCobB. Western blot analysis was done using anti-ACS primary antibody. OsCobB was found to bind physically to nuclear ACS. b*)* Kinetic parameters of NAD^+ as a cofactor for OsCobB deacylase activity of ACS was measured using nuclear extract containing ACS. Reactions were carried out with 0-800 µM NAD^+ with constant concentration of the substrates. ± indicate S.D; n=3. The MM plot shows the kinetics of the substrate using varied concentrations of NAD^+ (0-600 µM). The resultant plot was calculated using Graphpad Prism 9.3.0. The error bar depicts the S.D.; n=3. Further kinetic parameters (K_m and k_{cat} values) were calculated using the plot. OsCobB seems to have a preference for desuccinylation rather than deacetylation of ACS protein as indicated by the higher k_{cat}/K_m values.

2.2.2 Search for mitochondrial substrates of OsCobB

OsCobB was found to physically interact with mitochondrial proteins ACS (Acetyl CoA synthetase) (OsI_15767) and IDH2 (Isocitrate dehydrogenase) (OsI_16326) both *in-vitro* and *in-vivo* **(Fig 11.a-b).** The interacting partners were checked for deacetylation by OsCobB and their kinetic parameters for NAD^+ were calculated. The K_M values for binding of the ACS_{Ac} protein was calculated to be 114 µM, which is higher than that of binding of $IDH2_{Ac}$ **(Fig 11c).** It was also seen to have a higher catalytic efficiency of deacetylation in mitochondrial protein, ACS (804 $M^{-1}s^{-1}$) than IDH2 (422 $M^{-1}s^{-1}$). Apart from deacetylation, OsCobB could desuccinylate both ACS (1197 $M^{-1}s^{-1}$) and IDH2 (455 $M^{-1}s^{-1}$), with efficiencies greater than that of deacetylation **(Table 5).** This was similar to the trend observed in SIRT5 where the catalytic efficiency is lowest for ACS deacetylation[12].

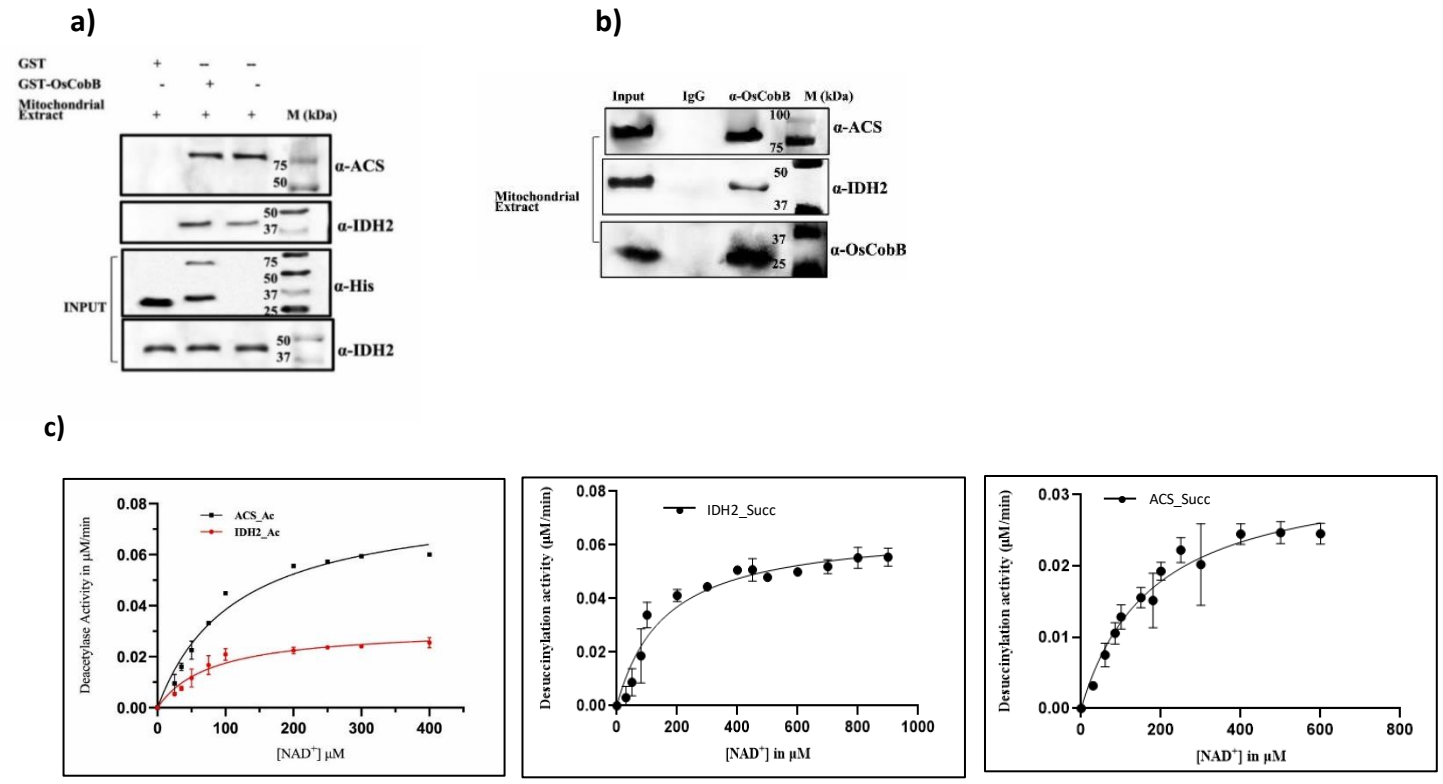

Fig 11. Mitochondrial substrates for OsCobB. a) Ni-NTA pull down assay was performed to find mitochondrial interacting partners for OsCobB. His-GST-tagged OsCobB (1µg) was interacted with leaf mitochondrial extract (30 µg). The resultant protein complexes were pulled down using Ni-NTA beads. Proteins were resolved on a 12% SDS-PAGE gel and western blot analysis was done using anti-ACS/IDH2 primary antibody to ascertain the identity of ACS and IDH2. b) Co-immunoprecipitation

assay showing the *in-vivo* interaction between OsCobB and the mitochondrial proteins, ACS and IDH2. 5µg of purified OscobB antibody was incubated with protein A/G beads followed by incubation with 1 mg mitochondrial extract. 5ug of IgG antibody was used as negative control. Western blot analysis was done using anti-AcS/IDH2 primary antibody. c) The MM plot showing the kinetics of acetylation and succinylation in ACS and IDH2 using varied concentrations of NAD^+ (0-600 µM). The resultant plot was calculated using Graphpad Prism 9.3.0. The error bar depicts the S.D.; n=3. Further kinetic parameters (K_m and k_{cat} values) were calculated using these plots. Reactions were carried out with 0-800 µM NAD^+ with constant concentration of the substrates. ± indicate S.D; n=3. d)

Substrate	**K_m for NAD^+ (µM)**	**k_{cat} (min^{-1})**	**k_{cat}/K_m (M^{-1} s^{-1})**
IDH2ac	79	2	422
IDH2succ	108	2.95	455
ACSac	114	5.5	804
ACSsucc	119.7	8.6	1197

Table 5- A comparison of the Michaelis Menten parameters for NAD^+ in OsCobB catalyzed acylation. Kinetic parameters for OscobB deacylase activity of ACS and IDH2 peptides was measured using dot blot method. Reactions were carried out with 0-800 µM NAD^+ with constant concentration of the peptides (1µg). The reaction mix was subjected to western blot analysis and their band intensities depicting the extent of deacylation measured in ImageJ. GST protein was added externally as a loading control. All the data were fitted into the MM plot using GraphPad Prism.

2.3 Exploration of the regulatory mechanism in OsCobB-associated deacylation processes.

Little has been known about the modulators of class III sirtuin enzymatic activity, although there are reports of product inhibition as a way of regulatory mechanism in sirtuins. Nicotinamide (NAM) acts as a potent inhibitor for numerous sirtuin-catalyzed deacylation activities, but it was found to be an ineffective inhibitor for OsCobB-catalyzed reaction. The IC_{50} value was calculated to be 253 ± 45µM indicating lower affinity of the enzyme towards NAM. Docking analysis with NAM shows the absence of interaction between Tyr55 and NAM due to the orientation of Tyr residue, which is essential for the inhibition activity as reported in SIRT5[56] **(Fig 12).**

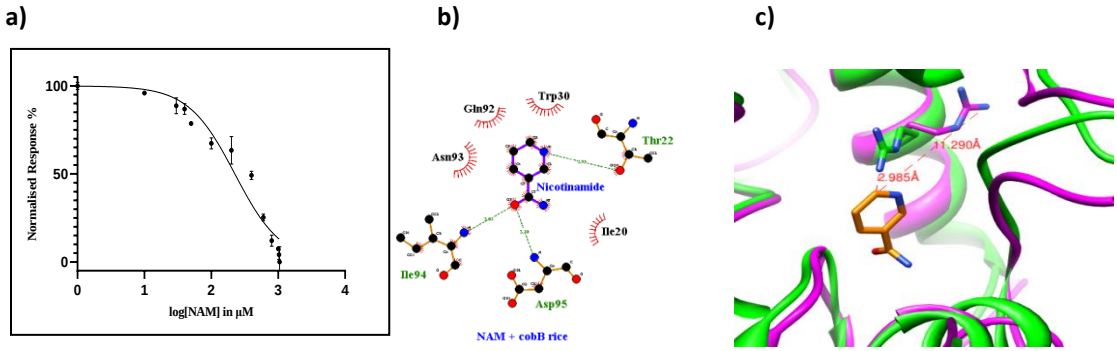

Fig 12. Inhibition studies with NAM in the deacetylation of H3K9ac peptide by OsCobB. a) Nicotinamide inhibition assay showing percentage changes in H3K9 deacetylation activity of OsCobB as a function of NAM concentration. b) Molecular docking analysis of OsCobB and nicotinamide (NAM) done in autodock vina and visualized in ligplot and Chimera software. The two-dimensional representation showed the absence of interaction between Tyr55 and NAM. Due to the orientation of the residue, there is an absence of any interaction between the two. SIRT5, shown in green ribbon representation, was seen to interact with NAM, which is responsible for effective inhibition in SIRT5. OsCobB bound to NAM was shown as magenta ribbon representation.

Further, the effect of different metal ions (Cu^{2+}, Ca^{2+}, Mg^{2+}, Mn^{2+}, Fe^{2+}) on the OsCobB-catalyzed deacetylation of histone H3 were analyzed. The deacetylation was majorly inhibited by Fe^{2+} and Mn^{2+} metal ions **(Fig. 13a)**. The inhibition mechanism is yet unknown but it reflects on the role of OsCobB in relation to metal ion stress and toxicity. Resveratrol, a natural polyphenol and activator of sirtuin catalyzed activities was seen to elevate OsCobB deacetylase activity by 50% at 51µM **(Fig. 13b).**

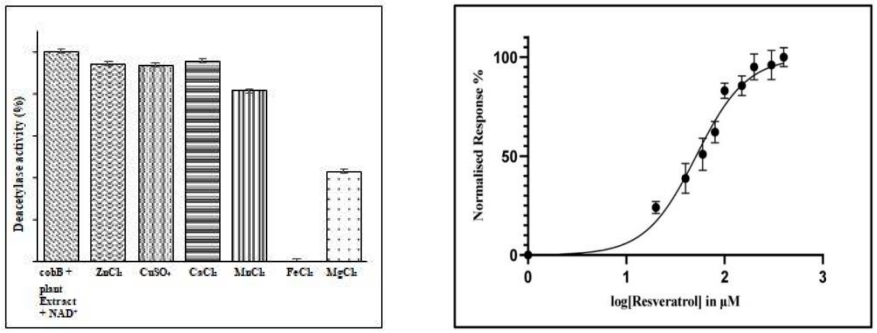

Fig 13. Effect of metal ion stress on deacetylation activity of OscobB. The bar graph compares the effect of metal ion-dependent deacetylation of histone H3 from nuclear extract. 0.5 mM concentration of each metal salts were used in the reaction

and their effects were deciphered using western blot analysis. The error bar depicts the S.D.; n=3. b) Effect of resveratrol as activator on OsCobB-catalyzed H3K9 deacetylation activity.

Objective 3- Insight into the biological significance of the protein under stress conditions

3.1 Role of OsCobB concerning histones during plant stress

We previously discovered that OsSRT1 was responsible for H3K9 deacetylation under oxidative stress, assisting in DNA repair[42]. Needless to say, OsCobB must be involved in other stress dependent regulation with respect to H3K9 deacetylation. To explore this idea, we compared the expression of OsCobB in the nucleus to the extent of acylation of its substrates to get an insight into its role in plant growth under different stress conditions The OsCobB expression was found to be 2.5 folds higher in the nucleus during low temperature and dehydration stress in comparison to the normal variety. At the same time, a decrease in the amount of H3K9ac under dehydration and low temperature conditions hints at the involvement of OsCobB in the deacetylation of histone H3K9 and further regulation of stress. The amount of H3K18ac was also seen to be significantly lower during dehydration stress **(Fig 14)**. Moreover, we also observed a 2-fold decrease in histone H3 butrylation and H4 succinylation in dehydration stress condition. H3K9 butrylation is usually enriched in transcription start sites and is known to be downregulated during dietary stress[60]. H3K9 acetylation is linked to lysine butrylation in realms of continuous darkness and anaerobic respiration[45]. H4 succinylation has also been documented to aid in DNA repair[61].During low temperature stress, we observed a 0.5 fold decrease in succinylation levels of both histones H3 and H4. At the same time, there was a 0.5 fold (approx.) decrease of acetylation, 2-hydroxyisobutrylation and b-hydroxybutrylation of histone H4.It would be interesting to further investigate the OsCobB regulation for the various stress stimuli. **(Fig 15).** This is also the first study to detect the presence of all these deacylations in plants.

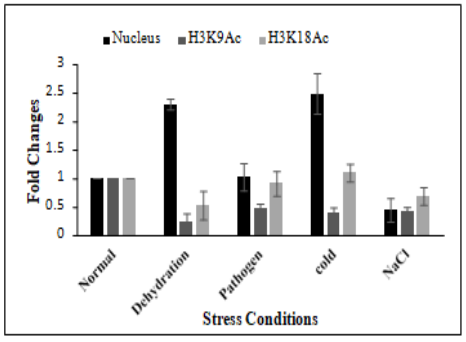

Fig 14. Comparative analysis of H3K9ac and H3K18aclevels and OscobB expression in different stress conditions. The bar graph compares the relationship between OscobB expression in nucleus in comparison to H3K9ac and H3K18ac levels under stress conditions. Western blot analysis was performed using H3K9ac and H3K18ac antibody to detect the intensity of its presence in those samples. Band intensities were measured using the ImageJ software and normalized to the loaded amount of H3.

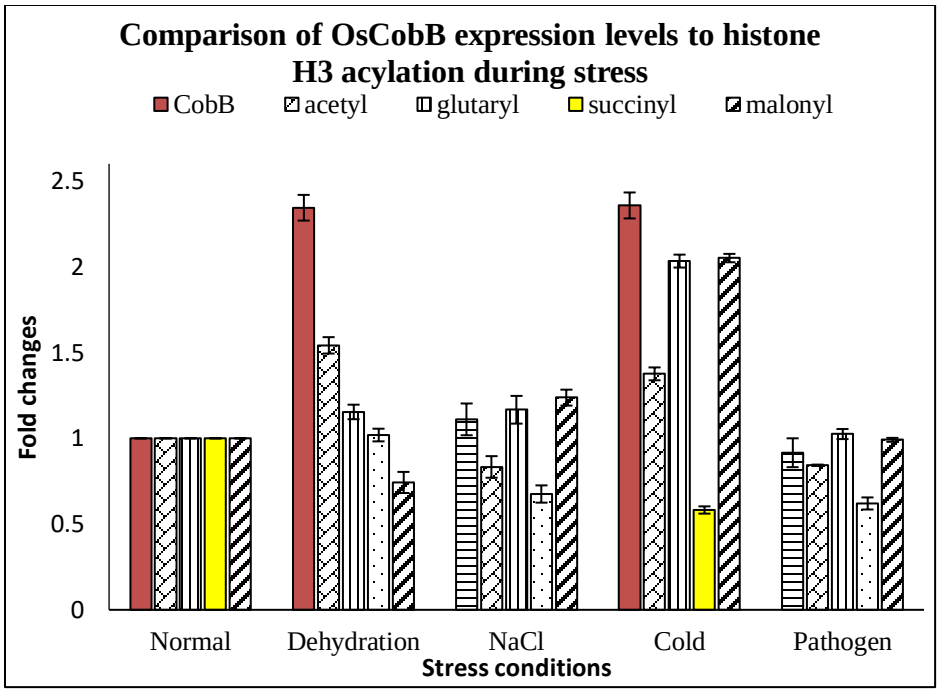

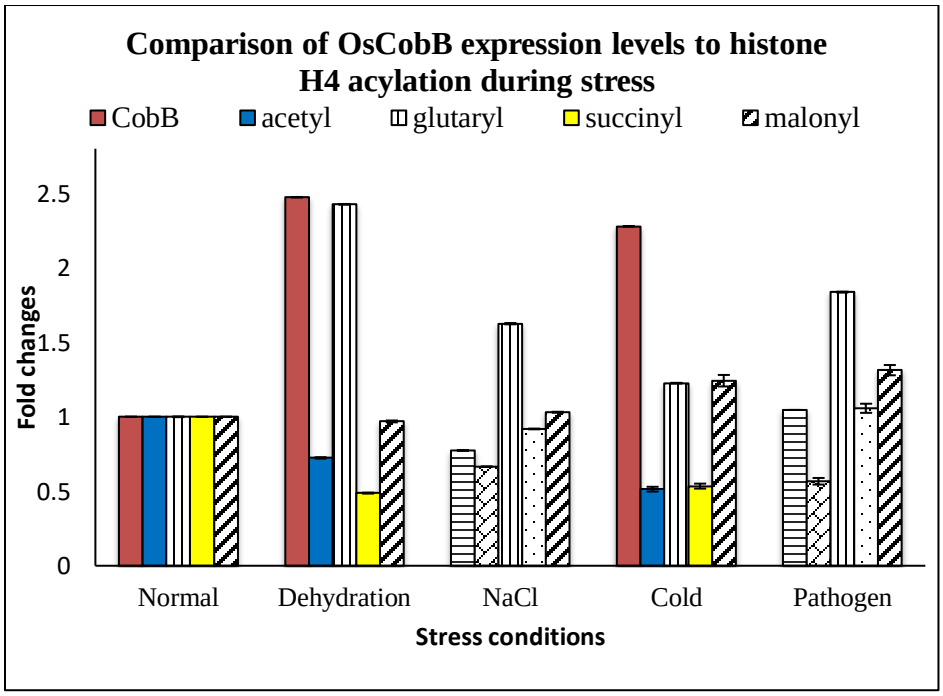

Fig.15- Detection of deacylation targets in histones H3 and H4 for OsCobB under stress conditions. Bar graph representation comparing the expression levels of OsCobB in comparison to levels of a) H3 b) H4 acylation in different plant stress conditions. Western blot analysis was used to detect the intensity of the acylation from leaf nuclear extract using acylation specific primary antibody. Loading control was analysed using anti-histone H3 primary antibody. The overexpression of OsCobB in the nucleus in times of dehydration and low temperature stress is correlated with elevated levels of H3 and H4 desuccinylation levels. Although, only H4 deacetylation could be linked to the two stress conditions. This emphasizes on the role of OsCobB desuccinylase and deacetylase activity in response to freezing temperatures and drought conditions.

3.2 Regulatory role of OsCobB in mitochondria

OsCobB- catalyzed IDH2 deacetylation plays a crucial role in TCA cycle in plants. IDH2 deacetylated at K391 (conserved as K413 in human SIRT3) is responsible for the dehydrogenation of isocitrate to oxalosuccinate in the mitochondria[62]. The deacetylation of IDH2 by SIRT3 was, in turn, linked to protection against oxidative damage[62]. Since OsCobB can both deacetylate and desuccinylate IDH2, we were interested to know its role during stress. In our experiments, the upregulation of OsCobB protein in the mitochondria is linked to low temperature, high salinity and pathogen stress. Furthermore, we observed a 2-fold increase in IDH2 deacetylation in low temperature stress while a 5 fold increase in IDH2 desuccinylation under pathogen stress **(Fig 16)**. Further, we performed an *in-vitro* isocitrate dehydrogenation assay using mitochondrial extract containing IDH2, both in the presence and absence of OsCobB and measured the NADPH released in the process in spectrophotometer at A340 nm. There was a 3-fold increase in the amount of NADPH released when OsCobB was involved in deacetylation of IDH2 prior to its enzymatic reaction. It hints at the fact that OsCobB is involved in the deacetylation of IDH2 in mitochondria, resulting in the activation of the enzyme and the subsequent conversion **(Fig 17).**

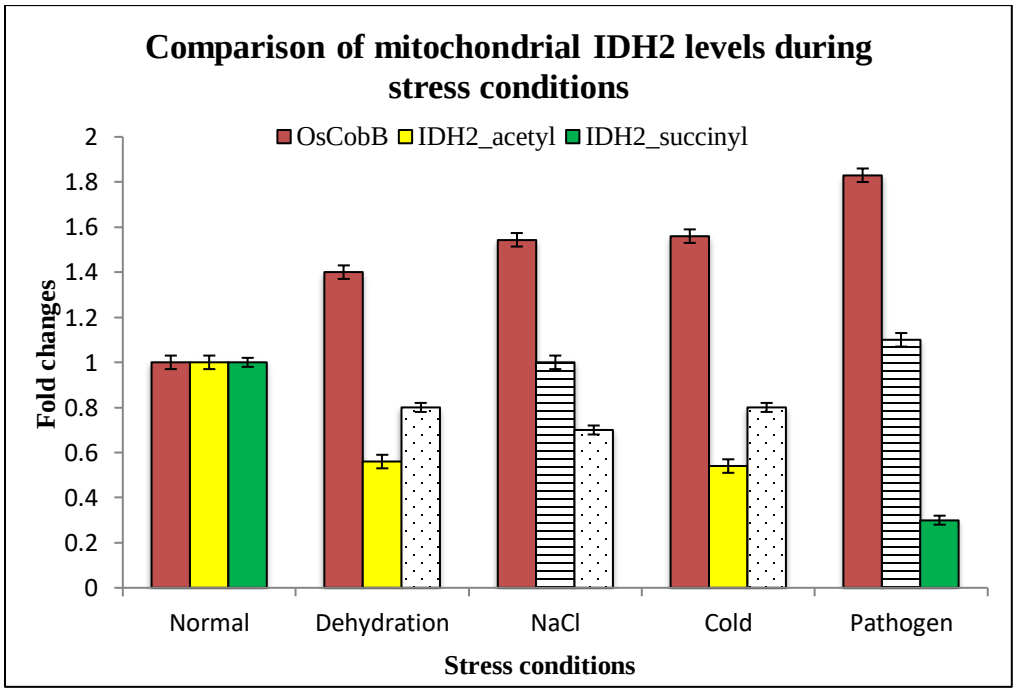

Fig 16. Preference of deacetylase and desuccinylase activities of IDH2 under stress conditions. a) Bar graph representation comparing the relationship between OscobB expression in comparison to IDH2 acylation levels under stress conditions. The

brown bars highlight the stress conditions in which OsCobB expression is elevated in mitochondrial fraction in comparison to normal rice varieties and thus is our stress of interest.

a)

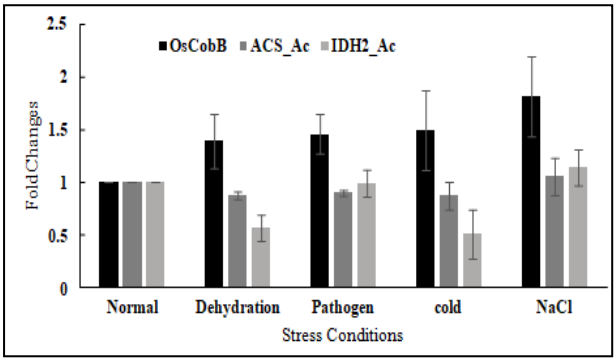

b)

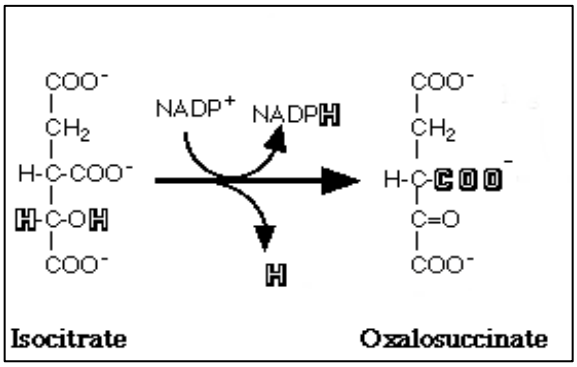

c)

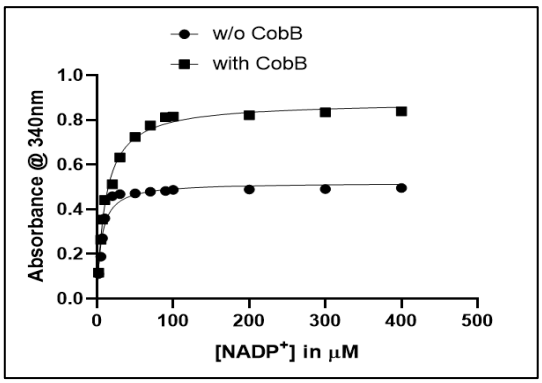

OsIDH2 activity	**Kinetic parameters**	**Isocitrate**	**$NADP^+$**
Without OsCobB	*Km* (µM)	0.8	2.8
	Vmax (mM/min/µg)	0.032 ± 0.001	0.037 ± 0.001
With OsCobB	*Km* (µM)	0.1	1.5
	Vmax (mM/min/µg)	0.1 ± 0.002	0.1 ± 0.002

Fig 17. Regulatory role of OscobB in the oxidation reaction of isocitrate involving IDH2. a) The bar graph compares the relationship between OscobB expression in mitochondria in comparison to ACSac and IDH2ac levels under stress conditions. b) The enzymatic reaction of dehydrogenation of isocitrate to oxalosuccinate catalyzed by deacetylated IDH2 (K256). c) The comparative analysis of the oxidative reaction of isocitrate in the presence and absence of OscobB. The IDH2 activity was measured in spectrophotometer at 340nm, the absorption maxima of NADPH.

ACS is another identified mitochondrial substrate for OsCobB found to be deacetylated and desuccinylated at position K667. According to a current report in *Arabidopsis*, deacetylation of ACS at K622 resulted in a 500 fold (approx.) increase in its activity[63]. Though the protein accountable for the change was not reported, it was assumed to be involved in maintaining acetate homeostasis. K622 residue was found to be conserved in OsACS as well apart from

sharing an 82% sequence identity with that of AtACS, hypothesizing the involvement of OsCobB in countering certain stress conditions by deacetylation of ACS. We have previously noted the deacetylation ability of OsCobB at nuclear ACS-K667 (homologous to mitochondrial ACS-K622) and therefore, have sought to test the same for the activation of the enzyme. Steady state kinetic analysis of ACS activity using both mitochondrial and nuclear ACS resulted in a 3-fold increase in the rate of conversion of acetate to acetyl-CoA in the presence of OsCobB **(Fig 18)**. Previously, ACSS2 expression was recognized to be upregulated during hypoxia and glucose deficient conditions in the mitochondria. It becomes apparent that under varied stresses, OsCobB is involved in the deacetylation of ACS in these organelles, resulting in the activation of the enzyme and the subsequent conversion of acetate.

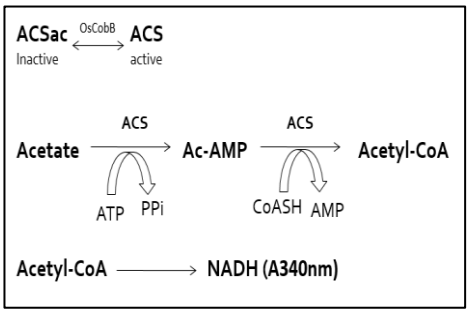

OsACS activity	**Kinetic parameters**	**Acetate (Mitochondrial ACS)**	**Acetate (Nuclear ACS)**
Without OsCobB	*Km* (mM)	76.55	47.89
	Vmax (mM/min/μg)	0.035 ±0.002	0.050±0.001
With OsCobB	*Km* (mM)	20.5	19.65
	Vmax (mM/min/μg)	0.018 ±0.001	0.018±0.001

Fig 18**. Regulatory role of OscobB in the synthesis of Acetyl CoA involving ACS.** a) The enzymatic reaction catalyzed by deacetylated ACS (K609). b) The comparative analysis of synthesis of Acetyl CoA and its subsequent conversion into NADH in the presence and absence of OscobB. The NADH produced was measured in spectrophotometer at 340nm, the absorption maxima of NADH.

Due to the dual localization of OsCobB, it is also possible for the protein to translocate between mitochondria and nucleus in order to deacylate ACS. In case of high salinity stress, there was a 1.8 fold increase in OsCobB expression in the mitochondria while the nuclear counterpart

remained lower than in normal conditions. This may be linked to ACS deacetylation as observed by the lowering of acetylation levels of mitochondrial ACS. This also hints at the probability of translocation of the protein from mitochondria to the nucleus during high saline conditions. We also observed an increase in mitochondrial OsCobB during dehydration stress that can be linked to ACS deacetylation as seen by the 5-fold decrease in acetylation of ACS **(Fig 19).**

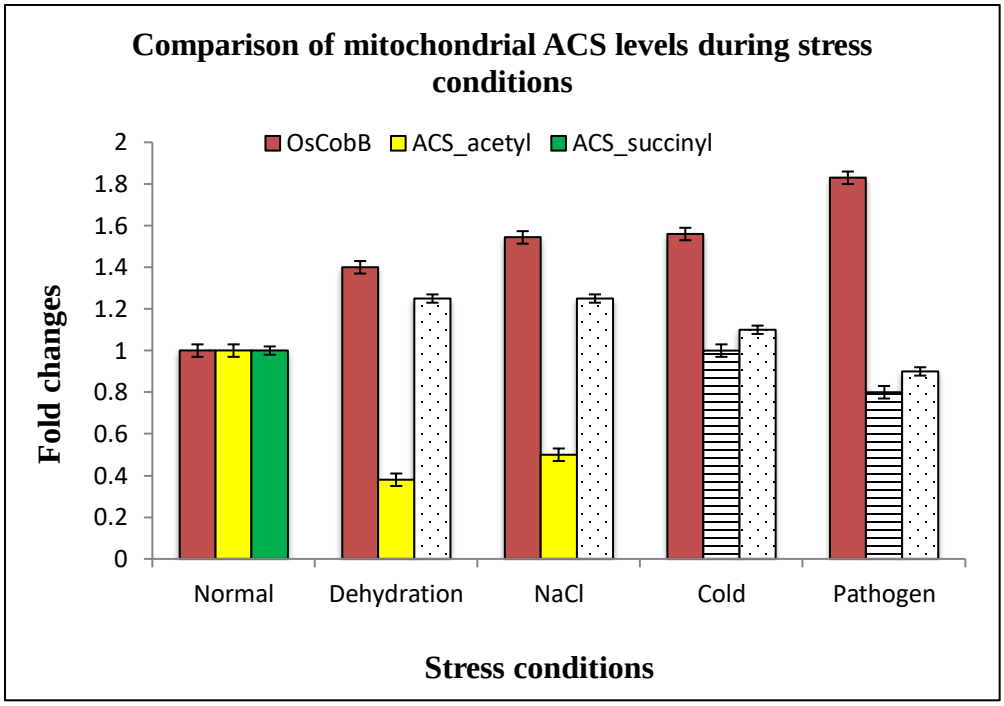

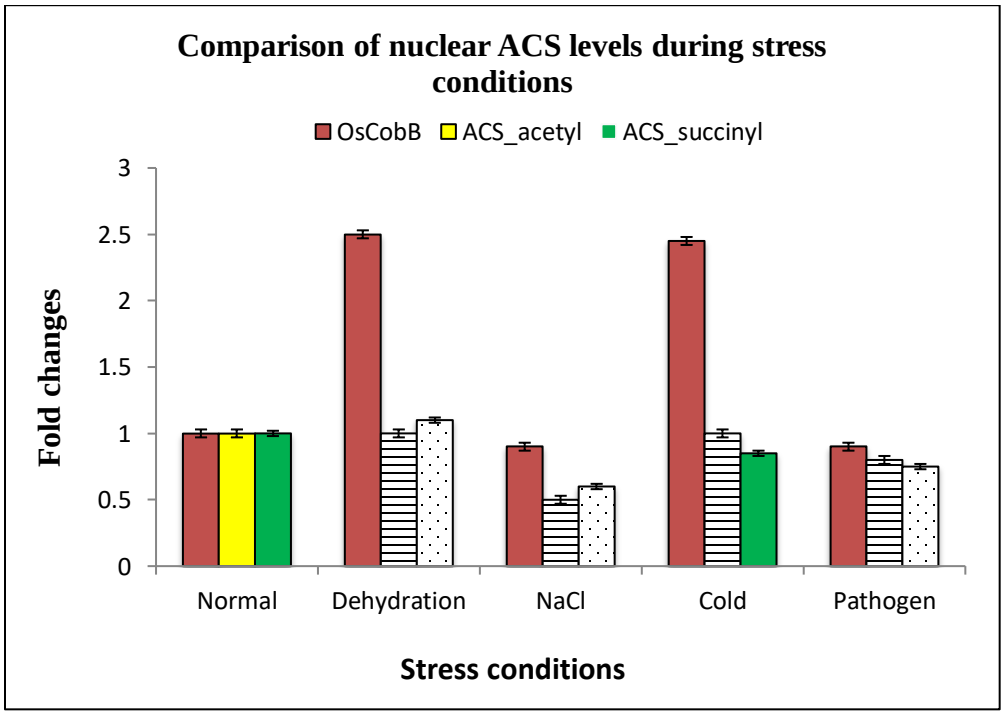

Fig 19. Comparative study of mitochondrial ACS deacetylase and desuccinylase levels in relation to OsCobB expression. Bar graph representation comparing the relationship between OscobB expression in comparison to ACS deacylation levels under stress conditions. Overexpression of OsCobB in mitochondria can be linked to ACS deacetylation during dehydration and high salinity stress.

6. Conclusion

In this study, OsCobB was discovered to be the first reported class III sirtuin in *Oryza sativa var indica*. OsCobB has the highest sequence identity with bacterial sirtuin, CobB, which is localized in the cytosol. OsCobB has been reported to be majorly localized in the mitochondria but is speculated to be overexpressed in the nucleus under stress conditions such as high salinity, in order to cope with the stress. OsCobB displays a number of deacylase activities regulating different proteins that can be linked to different stress conditions which the plant encounters during growth stage. However, this protein does not possess ADP-ribosyl transferase activity as seen in a few members of bacterial class III sirtuins[2,64]. OsCobB has a preference of deacetylation at H3K9ac position, rather than H3K18ac position due to the presence of strong hydrogen bond formation with Val151 residue in case of histone H3K9. OsSRT1, a nuclear sirtuin in *O.sativa var indica*, also plays a major role in warding off oxidative stress conditions by deacetylation at H3K9 position[42]. We found a correlation between H3K9 deacetylation and dehydration and low temperature stress conditions in case of OsCobB. Additionally, upregulation of nuclear OsCobB expression in times of low water availability was also connected to increased debutrylation of histone H3 and desuccinylation of histone H4. These modifications may have a role in warding off the stress. On the contrary, OsCobB-catalyzed H3 desuccinylation may be linked to H4 de-2-hydroxyisobutrylation and de-ß-hydroxybutrylation during cold stress. Kinetically, this enzyme has the ability to accommodate all modifications with a preference towards succinyl, malonyl and glutaryl side chains. The presence of Tyr55 and Arg58 residues in OsCobB assists in formation of strong bonds with negatively charged acyl side chains like that of succinyl and malonyl. Nicotinamide (NAM), a by-product of the sirtuin-catalysed deacylation reaction, often acts as a product inhibitor for the reaction[56]. However, NAM showed very weak product inhibiton. On the other hand, Fe^{2+} and Mn^{2+} ions seemed to greatly affect the OsCobB catalysed deacetylation reaction of histone H3.

OsCobB interacts with the mitochondrial proteins, ACS and IDH2 and can both deacetylate and desuccinylate the substrates. In presence of OsCobB, the IDH2 deacetylation activity increased 3-fold, using $NADP^+$ for its activity. From the stress response studies, we concluded that overexpression of OsCobB could be linked to IDH2 deacetylation under dehydration and low temperature stress. Thus, this regulation may be involved in maintaining $NADP^+$ homeostasis to cope these plant stresses. It would also be interesting to find the metabolic pathway regulated by desuccinylation of IDH2 by OsCobB under extreme saline conditions as found in our study.

Interestingly, OsCobB interacts with both the nuclear and mitochondrial ACS, facilitating its deacetylation and desuccinylation at K609. We observed a 2-fold increase in ACS deacetylation and 3-fold increase in ACS desuccinylation in the presence of OsCobB which may be a pre-requisite for defending against stresses. Though no prominent stress factors were found in connection to ACS desuccinylation, it is possible that OsCobB copes with high salinity stress by overexpressing itself in the mitochondria and lowering its expression in the nucleus, regulating ACS deacetylation and its subsequent pathways. Deacetylation of mitochondrial ACS could also be connected to protection against drought conditions.

This study brings to light the stress conditions in association to the deacylation targets in rice. However, it is essential in future to find the exact regulation of these deacylations in connection to plant stresses.

7. Future directions

OsCobB is the only reported class III sirtuin member in plants. Protein analysis against kingdom plantae has indicated the presence of this protein, though not reported yet. Western blot analysis using anti-OsCobB primary antibody against whole protein extracts from different plant leaves like tomato, brinjal, carrot, radish and spinach has hinted at the presence of this protein in plants as well. This opens new doors for exploration of class III sirtuins in plants and their role in different stress evasion. It is seen that OsCobB can colocalize in both mitochondria and nucleus under different stress conditions. Since no nuclear localization signal was found on OsCobB, there might be involvement of numerous transporter proteins aiding in the translocation. It would be very helpful to discover the transporter protein as it would give a better direction towards understanding the role of OsCobB in regulation different metabolic pathways. Also since NAM

did not pose to be an effective inhibitor, it would be beneficial to look for other potent inhibitors for OsCobB. Various deacetylation activities are discovered for OsCobB associated with DNA repair and transcription regulation during iron and manganese toxicity in the soil and drought stress conditions, although their regulatory mechanism is not yet established. Hence, this can potentially be a sphere to be investigated in the future.

8. Reference

1. Frye, R. A. Phylogenetic Classification of Prokaryotic and Eukaryotic Sir2-like Proteins. *Biochem. Biophys. Res. Commun.* **273**, 793–798 (2000).
2. Frye, R. A. Characterization of five human cDNAs with homology to the yeast SIR2 gene: Sir2-like proteins (Sirtuins) metabolize NAD and may have protein ADP-ribosyltransferase activity. *Biochem. Biophys. Res. Commun.* **260**, 273–279 (1999).
3. Rajabi, N. *et al.* Mechanism-Based Inhibitors of the Human Sirtuin 5 Deacylase: Structure-Activity Relationship, Biostructural, and Kinetic Insight. *Angew. Chemie Int. Ed.* **56**, 14836–14841 (2017).
4. Chen, Y. *et al.* Lysine propionylation and butyrylation are novel post-translational modifications in histones. *Mol. Cell. Proteomics* **6**, 812–819 (2007).
5. Colak, G. *et al.* Identification of Lysine Succinylation Substrates and the Succinylation Regulatory Enzyme CobB in *Escherichia coli*. *Mol. Cell. Proteomics* (2013) doi:10.1074/mcp.M113.031567.
6. Tan, M. *et al.* Identification of 67 histone marks and histone lysine crotonylation as a new type of histone modification. *Cell* **146**, 1016–1028 (2011).
7. Xie, Z. *et al.* Lysine Succinylation and Lysine Malonylation in Histones. *Mol. Cell. Proteomics* **11**, 100–107 (2012).
8. Peng, C. *et al.* The First Identification of Lysine Malonylation Substrates and Its Regulatory Enzyme. *Mol. Cell. Proteomics* **10**, M111.012658 (2011).
9. Wang, F. *et al.* SIRT5 Desuccinylates and Activates Pyruvate Kinase M2 to Block Macrophage IL-1β Production and to Prevent DSS-Induced Colitis in Mice. *Cell Rep.* **19**, 2331–2344 (2017).
10. Tan, M. *et al.* Lysine glutarylation is a protein posttranslational modification regulated by SIRT5. *Cell Metab.* **19**, 605–17 (2014).
11. Zhilhoung, Z. *et al.* Identification of lysine succinylation as a new post-translational modification. *Nat. Chem. Biol.* **7**, 58–63 (2011).
12. Du, J. *et al.* Sirt5 is a NAD-dependent protein lysine demalonylase and desuccinylase. *Science* **334**, 806–9 (2011).
13. Zhu, A. Y. *et al.* Plasmodium falciparum Sir2A preferentially hydrolyzes medium and

long chain fatty acyl lysine. *ACS Chem. Biol.* (2012) doi:10.1021/cb200230x.

14. Agnes L.C. Ong, T. S. R. Role of Sirtuin1-p53 regulatory axis in aging, cancer and cellular reprogramming. *Ageing Res. Rev.* **43**, 64–80 (2018).
15. Yasuda, T. & Takizawa, K. Genes to Cells Human SIRT2 and SIRT3 deacetylases function in DNA homologous recombinational repair. 328–335 (2021) doi:10.1111/gtc.12842.
16. Bao, X. *et al.* Identification of 'erasers' for lysine crotonylated histone marks using a chemical proteomics approach. *Elife* **3**, 1–18 (2014).
17. Mathias, R. A. *et al.* Sirtuin 4 is a lipoamidase regulating pyruvate dehydrogenase complex activity. **159**, 1615–1625 (2015).
18. Colak, G. *et al.* Identification of lysine succinylation substrates and the succinylation regulatory enzyme CobB in escherichia coli. *Mol. Cell. Proteomics* **12**, 3509–3520 (2013).
19. Starai, V. J. Sir2-Dependent Activation of Acetyl-CoA Synthetase by Deacetylation of Active Lysine. *Science (80-.).* **298**, 2390–2392 (2002).
20. Dong, H. *et al.* Protein lysine de-2-hydroxyisobutyrylation by CobB in prokaryotes. *Sci. Adv.* **5**, eaaw6703 (2019).
21. Li, R. *et al.* CobB regulates Escherichia coli chemotaxis by deacetylating the response regulator CheY. *Mol. Microbiol.* **76**, 1162–1174 (2010).
22. Gardner, J. G. & Escalante-Semerena, J. C. In Bacillus subtilis, the Sirtuin Protein Deacetylase, Encoded by the srtN Gene (Formerly yhdZ), and Functions Encoded by the acuABC Genes Control the Activity of Acetyl Coenzyme A Synthetase. *J. Bacteriol.* **191**, 1749–1755 (2009).
23. Garrity, J., Gardner, J. G., Hawse, W., Wolberger, C. & Escalante-Semerena, J. C. N - Lysine Propionylation Controls the Activity of Propionyl-CoA Synthetase. *J. Biol. Chem.* **282**, 30239–30245 (2007).
24. Lu, Y. *et al.* Dynamics and functional interplay of histone lysine butyrylation, crotonylation, and acetylation in rice under starvation and submergence. *Genome Biol.* **19**, (2018).
25. Khan, S., Mitra, N. & Dey, S. A CobB like sirtuin in Oryza sativa indica regulates the mitochondrial machinery under stress conditions. *Arch. Biochem. Biophys.* **731**, (2022).
26. Peng, C. *et al.* The First Identification of Lysine Malonylation Substrates and Its Regulatory Enzyme. *Mol. Cell. Proteomics* (2011) doi:10.1074/mcp.M111.012658.
27. Avalos, J. L. *et al.* Structure of a Sir2 enzyme bound to an acetylated p53 peptide. *Mol. Cell* **10**, 523–535 (2002).
28. Zhou, L. *et al.* SIRT 5 promotes IDH 2 desuccinylation and G6 PD deglutarylation to enhance cellular antioxidant defense . *EMBO Rep.* (2016) doi:10.15252/embr.201541643.
29. Michishita, E. *et al.* SIRT6 is a histone H3 lysine 9 deacetylase that modulates telomeric chromatin. *Nature* (2008) doi:10.1038/nature06736.
30. Yu, W., Dittenhafer-Reed, K. E., Denu, J. M. & Eric C. Meyers, Bleyda R. Solorzano,

Justin James, Patrick D. Ganzer, Elaine S., Robert L. Rennaker, M. P. K. and S. H. Sirt6 regulates TNFα secretion via hydrolysis of long chain fatty acyl lysine. *J. Biol. Chem.* **287**, 14078–14086 (2018).

31. Yang, S. J. *et al.* Activation of Peroxisome Proliferator-Activated Receptor Gamma by Rosiglitazone Increases Sirt6 Expression and Ameliorates Hepatic Steatosis in Rats. **6**, (2011).

32. Wu, Y. *et al.* Overexpression of Sirtuin 6 suppresses cellular senescence and NF- κ B mediated inflammatory responses in osteoarthritis development. *Nat. Publ. Gr.* 1–11 (2015) doi:10.1038/srep17602.

33. Vassilopoulos, A., Fritz, K. S., Petersen, D. R. & Gius, D. The human sirtuin family : Evolutionary divergences and functions. **5**, 485–496 (2011).

34. Barber, M. F. *et al.* SIRT7 links H3K18 deacetylation to maintenance of oncogenic transformation. *Nature* **487**, 114–118 (2013).

35. Li, L. *et al.* SIRT7 is a histone desuccinylase that functionally links to chromatin compaction and genome stability. *Nat. Commun.* **7**, 1–17 (2016).

36. Simonet, N. G. *et al.* SirT7 auto-ADP-ribosylation regulates glucose starvation response through mH2A1. *Sci. Adv.* **6**, 1–16 (2020).

37. Yu, A. Q. *et al.* SIRT7-Induced PHF5A Decrotonylation Regulates Aging Progress Through Alternative Splicing-Mediated Downregulation of CDK2. *Front. Cell Dev. Biol.* **9**, 1–15 (2021).

38. Busconi, M., Reggi, S., Fogher, C. & Bavaresco, L. Evidence of a sirtuin gene family in grapevine (Vitis vinifera L.). *Plant Physiol. Biochem. PPB* **47**, 650–2 (2009).

39. Wang, C. *et al.* Arabidopsis putative deacetylase AtSRT2 regulates basal defense by suppressing PAD4, EDS5 and SID2 expression. *Plant Cell Physiol.* **51**, 1291–9 (2010).

40. Zhao, L. *et al.* Identification and characterization of histone deacetylases in tomato (Solanum lycopersicum). *Front. Plant Sci.* **5**, (2015).

41. Zhen, S. *et al.* First Comprehensive Proteome Analyses of Lysine Acetylation and Succinylation in Seedling Leaves of Brachypodium distachyon L. *Sci. Rep.* **6**, 1–15 (2016).

42. Huang, L. *et al.* Down-Regulation of a SILENT INFORMATION REGULATOR2-Related Histone Deacetylase Gene, OsSRT1, Induces DNA Fragmentation and Cell Death in Rice. *Plant Physiol.* **144**, 1508–1519 (2007).

43. Zhong, X. *et al.* The Rice NAD+-Dependent Histone Deacetylase OsSRT1 Targets Preferentially to Stress- and Metabolism-Related Genes and Transposable Elements. *PLoS One* **8**, e66807 (2013).

44. Zhang, H., Zhao, Y. & Zhou, D.-X. Rice NAD+-dependent histone deacetylase OsSRT1 represses glycolysis and regulates the moonlighting function of GAPDH as a transcriptional activator of glycolytic genes. *Nucleic Acids Res.* **45**, 12241–12255 (2017).

45. Lu, Y. *et al.* Dynamics and functional interplay of histone lysine butyrylation, crotonylation, and acetylation in rice under starvation and submergence. *Genome Biol.*

(2018) doi:10.1186/s13059-018-1533-y.

46. Yuan, H. & Marmorstein, R. Structural Basis for Sirtuin Activity and Inhibition. *J. Biol. Chem.* **287**, 42428–42435 (2012).

47. Ringel, A. E., Roman, C. & Wolberger, C. Alternate deacylating specificities of the archaeal sirtuins Sir2Af1 and Sir2Af2. *Protein Sci.* **23**, 1686–1697 (2014).

48. Fukasawa, Y. *et al.* MitoFates: Improved prediction of mitochondrial targeting sequences and their cleavage sites. *Mol. Cell. Proteomics* **14**, 1113–1126 (2015).

49. Rakesh Kaundal, G. P. S. R. D. RSLpred: an integrative system for predicting subcellular localization of rice proteins combining compositional and evolutionary information. *Proteomics Syst. Biol.* **9**, 2324–2342 (2009).

50. Olof Emanuelsson, Søren Brunak, G. von H. & H. N. Locating proteins in the cell using TargetP, SignalP and related tools. *Nat. Protoc.* **2**, 953–971 (2007).

51. Scher, M. B., Vaquero, A. & Reinberg, D. SirT3 is a nuclear NAD+-dependent histone deacetylase that translocates to the mitochondria upon cellular stress. *Genes Dev.* **21**, 920–8 (2007).

52. Matsushita, N. *et al.* Distinct regulation of mitochondrial localization and stability of two human Sirt5 isoforms. *Genes to Cells* (2011) doi:10.1111/j.1365-2443.2010.01475.x.

53. Avalos, J. L. *et al.* Structure of a Sir2 Enzyme Bound to an Acetylated p53 Peptide. *Mol. Cell* **10**, 523–535 (2002).

54. Chang, J.-H. *et al.* Structural Basis for the NAD-dependent Deacetylase Mechanism of Sir2. *J. Biol. Chem.* **277**, 34489–34498 (2002).

55. Rardin, M. J. *et al.* SIRT5 regulates the mitochondrial lysine succinylome and metabolic networks. *Cell Metab.* (2013) doi:10.1016/j.cmet.2013.11.013.

56. Fischer, F. *et al.* Sirt5 Deacylation Activities Show Differential Sensitivities to Nicotinamide Inhibition. *PLoS One* (2012) doi:10.1371/journal.pone.0045098.

57. Xu, H., Hegde, S. S. & Blanchard, J. S. Reversible acetylation and inactivation of Mycobacterium tuberculosis acetyl-CoA synthetase is dependent on cAMP. *Biochemistry* (2011) doi:10.1021/bi200156t.

58. Li, X. *et al.* Nucleus-Translocated ACSS2 Promotes Gene Transcription for Lysosomal Biogenesis and Autophagy. *Mol. Cell* **66**, 684-697.e9 (2017).

59. Hallows, W. C., Lee, S. & Denu, J. M. Sirtuins deacetylate and activate mammalian acetyl-CoA synthetases. *Proc. Natl. Acad. Sci. U. S. A.* **103**, 10230–10235 (2006).

60. Yang, Z., He, M., Austin, J., Pfleger, J. & Abdellatif, M. Histone H3K9 butyrylation is regulated by dietary fat and stress via an Acyl-CoA dehydrogenase short chain-dependent mechanism. *Mol. Metab.* **53**, 1–16 (2021).

61. Shi, R. *et al.* Succinylation at a key residue of FEN1 is involved in the DNA damage response to maintain genome stability. *Am. J. Physiol. - Cell Physiol.* **319**, C657–C666 (2020).

62. Yu, W., Dittenhafer-Reed, K. E. & Denu, J. M. SIRT3 protein deacetylates isocitrate

dehydrogenase 2 (IDH2) and regulates mitochondrial redox status. *J. Biol. Chem.* **287**, 14078–14086 (2012).

63. Naazneen Sofeo, Karina Leung, B. J. N. Modulation of plant Acetyl CoA Synthetase activity by acetylation. (2020).

64. Tsang, A. W. & Escalante-Semerena, J. C. CobB, a new member of the SIR2 family of eucaryotic regulatory proteins, is required to compensate for the lack of nicotinate mononucleotide:5,6-dimethylbenzimidazole phosphoribosyltransferase activity in cobT mutants during cobalamin biosynthesis in Salm. *J. Biol. Chem.* **273**, 31788–94 (1998).

65. Avalos, J. L., Bever, K. M. & Wolberger, C. Mechanism of sirtuin nhibition by nicotinamide: Altering the NAD+cosubstrate specificity of a Sir2 enzyme. *Mol. Cell* **17**, 855–868 (2005).

66. Min, J., Landry, J., Sternglanz, R. & Xu, R.-M. Crystal Structure of a SIR2 Homolog–NAD Complex. *Cell* **105**, 269–279 (2001).

67. Tucker, A. C. & Escalante-Semerena, J. C. Biologically active isoforms of CobB sirtuin deacetylase in Salmonella enterica and Erwinia amylovora. *J. Bacteriol.* **192**, 6200–6208 (2010).

68. Colak, G. *et al.* Identification of Lysine Succinylation Substrates and the Succinylation Regulatory Enzyme CobB in Escherichia coli. *Mol. Cell. Proteomics* **12**, 3509–3520 (2013).

69. Zhao, K., Chai, X. & Marmorstein, R. Structure and Substrate Binding Properties of cobB, a Sir2 Homolog Protein Deacetylase from Escherichia coli. *J. Mol. Biol.* (2004) doi:10.1016/j.jmb.2004.01.060.

70. Tsang, A. W. & Escalante-Semerenat, J. C. CobB, a new member of the SIR2 family of eucaryotic regulatory proteins, is required to compensate for the lack of nicotinate mononucleotide:5,6- dimethylbenzimidazole phosphoribosyltransferase activity in cobT mutants during cobalamin biosynthesis in Sal. *J. Biol. Chem.* **273**, 31788–31794 (1999).

71. Zhou, Y. *et al.* The bicyclic intermediate structure provides insights into the desuccinylation mechanism of human sirtuin 5 (SIRT5). *J. Biol. Chem.* (2012) doi:10.1074/jbc.M112.384511.

72. Wang, C. *et al.* CPT1A-mediated succinylation of S100A10 increases human gastric cancer invasion. *J. Cell. Mol. Med.* **23**, 293–305 (2019).

73. Wang, H. L. *et al.* Interactions between sirtuins and fluorogenic small-molecule substrates offer insights into inhibitor design. *RSC Adv.* (2017) doi:10.1039/c7ra05824a.

74. Szczepankiewicz, B. G. *et al.* Synthesis of carba-NAD and the structures of its ternary complexes with SIRT3 and SIRT5. *J. Org. Chem.* (2012) doi:10.1021/jo301067e.

75. Lin, Z.-F. *et al.* SIRT5 desuccinylates and activates SOD1 to eliminate ROS. *Biochem. Biophys. Res. Commun.* **441**, 191–195 (2013).

76. Sadhukhan, S. *et al.* Metabolomics-assisted proteomics identifies succinylation and SIRT5 as important regulators of cardiac function. *Proc. Natl. Acad. Sci. U. S. A.* **113**, 4320–4325 (2016).

77. Nishida, Y. *et al.* SIRT5 Regulates both Cytosolic and Mitochondrial Protein Malonylation with Glycolysis as a Major Target. *Mol. Cell* **59**, 321–332 (2015).

9. Plagiarism Certificate

Document Information

Analyzed document	Sonali_5000.docx (D171896177)
Submitted	2023-07-08 19:51:00
Submitted by	Sanghamitra Dey
Submitter email	sdey.dbs@presiuniv.ac.in
Similarity	0%
Analysis address	sdey.dbs.presi@analysis.urkund.com

Sources included in the report

Entire Document

Protein posttranslational modifications (PTMs) by lysine acylation are unfolding as a channel of metabolic regulations in response to critical environmental stress conditions. Sirtuins are the NAD^+- dependent deacylases that have been well-researched to play an important role in these PTMs in organisms ranging from prokaryotes to eukaryotes. However, plant sirtuins are still a lesser explored area. This work focuses on OsCobB that has been identified in Oryza sativa var indica as the only member of class III sirtuin family in plants. Besides, this protein has 89% sequence identity with the bacterial sirtuin, CobB. Thus, it would be interesting to explore the structural and biochemical aspects of a CobB-like protein in plants to better understand its biological roles. OsCobB is localized majorly in the mitochondria with traces present in the nucleus as well. Histones H3 and H4 are the nuclear targets for OsCobB, with a preference of deacetylation at H3K9 and H3K18 residues. Molecular simulation studies have confirmed that NAD+ binding is a pre-requisite for the effective binding of the substrate at the active site of OsCobB. The formation of a hydrophobic tunnel at the catalytic site is necessary for the proper incorporation of the acyl modification which would otherwise be loosely bound to the protein. Additionally, molecular docking analysis with H3K9 peptide linked to varied acylations predicted its preference of binding with succinyl, malonyl and glutaryl groups effectively. There is also a possibility of conformational changes at the active site for the incorporation of longer acyl side chains. This was further supported by in-vitro deacylase experiments with OsCobB. The interaction between the lysine modifications and Tyr55 and Arg58 residues of the protein strengthens the binding of the negatively charged acyl groups. No ADP ribosyl transferase activity was detected in OsCobB, in contrast to some of the class III members. The deacetylation of histone H3 was unstirred by its products, nicotinamide and ADP ribose but was sensitive to metal ions like Mg^{2+} and Fe^{2+}. In mitochondria, Isocitrate dehydrogenase (IDH2) was a target for deacetylation and desuccinylation at K391. IDH2 activity increased 2-fold in the presence of OsCobB which may have a pivotal role in responding to dehydration and low temperature stress. Surprisingly, Acetyl CoA Synthetase (ACS) was also found to be a substrate for OsCobB in both mitochondria and nucleus, capable of deacetylation as well as desuccinylation of the target protein. Additionally, mitochondrial ACS activity increased by 2-fold while the activity of nuclear ACS increased by 3-fold in the presence of OsCobB. This regulation might have a role to play in the nucleus by ACS desuccinylation during high saline conditions as there is an overexpression of OsCobB in the nucleus alongside a low expression of the same in mitochondria. Furthermore, histones H3 desuccinylation and debutrylation along with H4 desuccinylation and de-ß-hydroxybutrylation may be involved in adapting to low temperatures. On the other hand, desuccinylation of H4 with debutrylation of H3 played an important role in tolerance against dehydration stress. In this way, our study is the first to characterize the different deacylations in O.sativa var indica, both in-vivo as well as in-vitro. Sirtuins belong to
class III HDAC superfamily with NAD+-dependent deacylase and/or ADP ribosyltransferse activity,

10. Appendix

Table 6- List of antibodies

Sr no.	Antibody	Company	Catalog no.
1.	acetyl histone H3 Ab sampler kit	cell signaling technology	9927T
2.	acetylated histone H4 antibody sampler pack	abcam	ab218056
3.	anti-H4 antibody	abcam	ab177840
4.	anti-H3 antibody	biobharti	BB-AB0055
5.	anti-H2B antibody	abcam	ab1790
6.	acetylated lysine (ac-k-103) mouse mAb	cell signaling technology	9681S
7.	Rb pAb to Histone H3 (butyryl K9)	abcam	ab241248
8.	Rb mAb to Histone H3 (crotonyl K9)	abcam	ab271346
9.	Rb pAb to Histone H3 (propionyl K23)	abcam	ab241466
10.	Rb mAb to Histone H4 (beta-hydroxybutyryl K5)	abcam	ab243246
11.	Rb mAb to Histone H4 (butyryl K16)	abcam	ab240615
12.	Rb pAb to Histone H4 (propionyl K5)	abcam	ab241252
13.	Rb pAb to Histone H4 (propionyl K16)	abcam	ab240612
14.	Rb mAb to Histone H4 (crotonyl K8)	abcam	ab201075
15.	Rb mAb to Histone H4	abcam	ab177844
16.	Rb pAb to Histone H3 (acetyl K56)	abcam	ab195478
17.	Rb pAb to Histone H3 (acetyl K9)	abcam	ab10812
18.	Rb pAb to Histone H3 (acetyl K18)	abcam	ab1191
19.	Rb pAb to biotin (HRP)	abcam	ab53468
20.	Rb pAb toACSS2	abcam	ab66038
21.	IDH2 antibody	phyto ab	PHY0040S
22.	Rb anti-AOX1/2 plant	agrisera	AS04054
23.	goat anti mouse IgG-HRP Sec	santa cruz biotechnology	sc-2005
24.	Goat anti-rabbit IgG-HRP Sec	cell signaling	7074P2
25.	anti-GAPDH antibody	biobharti	BB-AB0060
26.	Rb pAb to K-malonylation (PAN)	PTM biolab	PTM-901
27.	Mouse mAb to K-succinylation (PAN)	PTM biolab	PTM-419
28.	anti Glutaryl lysine Ab (PAN)	PTM biolab	PTM-1152
29.	anti propionyl lysine Ab (PAN)	PTM biolab	PTM-201
30.	Tic40	agrisera	AS10709
31.	Catalase	agrisera	AS09501
32.	Rb pAb to untagged OsCobB antibody (Custom made)	BioBharti Lifesciences	

Table 7- List of peptides

Sr no.	Peptide	Company	Catalogue no.
1	Histone H4 recombinant protein	NEB	M2504S
2	Histone H3.1 recombinant protein	NEB	M2503S
3	Histone H2B recombinant protein	NEB	M2505S
4	Histone H2A recombinant protein	NEB	M2502S
5	Histone H1 recombinant protein	NEB	M2501S
6	human histone H3K9 peptide	abcam	ab16635
7	poly peptide ARTKQTARK(ace)STGG	bio basic	BGA003-1
8	ACS(ace) KTRSGK(ace)MRRI	ABclonal	Peptide0937
9	H3K9(mal) ARTKQTARK(mal)STGG	ABclonal	Peptide0936
10	H3K9(succ) ARTKQTARK(succ)STGG	Synthetic peptide	GTA70593-1
11	ACS(succ) KTRSGK(succ)IMRRI	Synthetic peptide	GTA70593-3
12	IDH2(succ) FTEGAFK(succ)DWGYQLAR	Synthetic peptide	GTA70593-4
13	H4K16(ace) KGLGKGGAK(ace)RHRKVLRD	Synthetic peptide	GTA70593-5
14	H3K9 (Myr) ARTKQTARK(myristoyl)STGG	Synthetic peptide	1011198
15	H3K9 (2HIB) ARTKQTARK(2-hydroxy isobutryl)STGG	Synthetic peptide	1011199
16	H3K9(glu) ARTKQTARK(glu)STGG	Synthetic peptide	GTA70671-1
17	H3K9(cro) ARTKQTARK(cro)STGG	Synthetic peptide	GTA70671-3
18	H3K9(pro) ARTKQTARK(prop)STGG	Synthetic peptide	GTA70671-2
19	H3K9(2-hydroxy isobutryl) ARTKQTARK(2HIB)STGG	Synthetic peptide	GTA70671-6
20	H3K9(mal) ARTKQTARK(mal)STGG	Synthetic peptide	GTA70671-5
21	H3K9(but) ARTKQTARK(but)STGG	Synthetic peptide	GTA70671-4

Table 4- Biological functions of class III sirtuins members

Protein	Organism	Substrate	Biological Activities mentioned
Sir2Af2	*A.flavidus*	p53	Deacetylation [65]
Sir2Af1	*A.flavidus*	BSA	Deacetylation [54]
Sir2Af1	*A.flavidus*	BSA	NAD-NAM exchange, deacetylation [66]
Sir2Af1,Sir2Af2	*A.flavidus*	H4K16	Desuccinylation Demyristoylation[47]
PfSir2A	*P.falciparum*	H3K9	Deacetylation, debutyrylation, deoctanoylation, and demyristoylation[13]
CobB	*S.enterica,* *E.amylovora*	ACS	Deacetylation [67]
CobB	*E.coli*	H3K9	Desuccinylation and deacetylation[68]
CobB	*E.coli*	ACS, H4	Deacetylation[69]
CobB	*E.coli*	ACS, CheY	Deacetylation [21]
CobB	*E.coli*	BSA	ADP- ribosylation[2]
CobB	*S.typhimurium*	Propionate	Catabolism property[70]
CobB	*S.typhimurium*		PRTase activity[23]
Sirt5	*H.sapiens*	H3K9, GDH, ACS2	Deacetylation, Demalonylation and desuccinylation[12]
Sirt5	*H.sapiens*	H3K9	Desuccinylation[71]
Sirt5	*H.sapiens*	S100A10	Desuccinylation[72]
Sirt5	*H.sapiens*	BKA	Desuccinylation[73]
Sirt5	*H.sapiens*	IDH2, G6PD	Desuccinylation, Deglutarylation[28]
Sirt5	*H.sapiens*	IDH2	Desuccinylation[74]
Sirt5	*H.sapiens*	SOD1	Desuccinylation[75]
Sirt5	*H.sapiens*	ACS2	Deacetylation [56]

Sirt5	*M.musculus*		Desuccinylation and fatty acid oxidation [55]
Sirt5	*M.musculus*	ECHA	Desuccinylation and fatty acid oxidation [76]
Sirt5	*M.musculus*	GAPDH-K184	Demalonylation and desuccinylation[77]

Additional documents

Certificate of Participation

This is to certify that

Sonali Khan

Presidency University, Kolkata

presented *POSTER* in the two day International Conference (Online) on

"Biomolecules To Biome" held on August 24-25, 2022

Organized by Department of Life Sciences, Presidency University, Kolkata, India.

Dr. Ranjana Pal & Dr. Puja Ray
Joint Organizing Secretaries
Biomolecules To Biome - 2022

Prof. Prabir Kumar Mukhopadhyay
HOD (Life Sciences)
Presidency University, Kolkata
(Chairman)

Prof. Sankar Bose
Dean of Faculty of Natural and Mathematical Sciences
(Patron)

MADURAI KAMARAJ UNIVERSITY
MADURAI-625021, TAMIL NADU
University with Potential for Excellence
(Re-accredited by NAAC with "A++" Grade in the 4th Cycle)

4th INTERNATIONAL CONFERENCE ON GENOME BIOLOGY (ICGB-4) & 54th ANNUAL AQUA-TERR DAY

FEBRUARY 28 & MARCH 1, 2023

Certificate of Participation

THIS IS TO CERTIFY THAT

Ms. Sonali Khan, Dept. of Life Sciences, Presidency University

participated and has made an poster presentation entitled " cobB - like protein - mystery behind the presence of a bacterial protein in plant, *Oryza sativa indica* " in the 4th International Conference on Genome Biology (ICGB- 4) & 54th Annual Aqua-Terr Day

Prof. S. Chandrasekaran
Convener

Dr. T. Jebasingh
Organizing Secretary

Dr. M. Jayalakshmi
Organizing Secretary

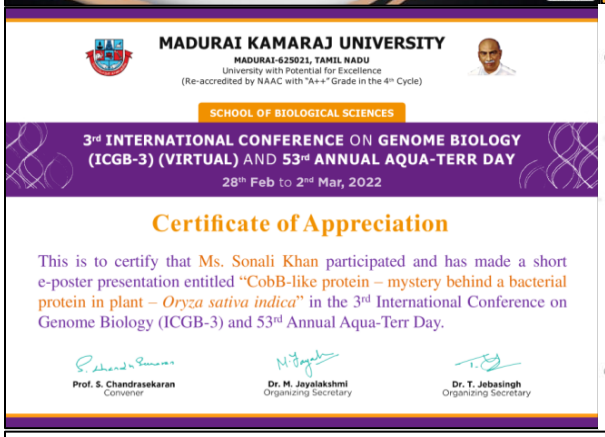

MADURAI KAMARAJ UNIVERSITY
MADURAI-625021, TAMIL NADU
University with Potential for Excellence
(Re-accredited by NAAC with "A++" Grade in the 4th Cycle)

SCHOOL OF BIOLOGICAL SCIENCES

3rd INTERNATIONAL CONFERENCE ON GENOME BIOLOGY (ICGB-3) (VIRTUAL) AND 53rd ANNUAL AQUA-TERR DAY

28th Feb to 2nd Mar, 2022

Certificate of Appreciation

This is to certify that Ms. Sonali Khan participated and has made a short e-poster presentation entitled "CobB-like protein – mystery behind a bacterial protein in plant – *Oryza sativa indica*" in the 3rd International Conference on Genome Biology (ICGB-3) and 53rd Annual Aqua-Terr Day.

Prof. S. Chandrasekaran
Convener

Dr. M. Jayalakshmi
Organizing Secretary

Dr. T. Jebasingh
Organizing Secretary

ONLINE SKILL DEVELOPMENT PROGRAM
on
IN-SILICO DRUG DESIGNING AND MOLECULAR DYNAMICS SIMULATIONS

13 – 19 NOVEMBER, 2021

@

GOOGLE MEET

CytoGene
Inventing Thoughts

ISO 9001 : 2015, ISO 14001 : 2015
ISO 45001:2018

CYTOGENE RESEARCH & DEVELOPMENT
LUCKNOW - 226021

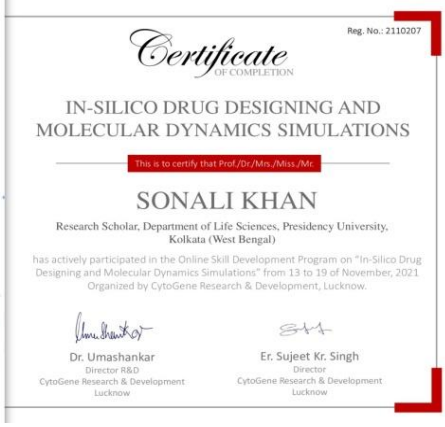

Reg. No.: 2110207

Certificate
OF COMPLETION

IN-SILICO DRUG DESIGNING AND MOLECULAR DYNAMICS SIMULATIONS

This is to certify that Prof./Dr./Mrs./Miss./Mr.

SONALI KHAN

Research Scholar, Department of Life Sciences, Presidency University, Kolkata (West Bengal)

has actively participated in the Online Skill Development Program on "In-Silico Drug Designing and Molecular Dynamics Simulations" from 13 to 19 of November, 2021 Organized by CytoGene Research & Development, Lucknow.

Dr. Umashankar
Director R&D
CytoGene Research & Development
Lucknow

Er. Sujeet Kr. Singh
Director
CytoGene Research & Development
Lucknow

National Virtual Conference
on
"Genomics to Phenomics: A New Horizon in Plant Science Research"
Organized by
Department of Botany, University of Calcutta

Certificate of Participation

This is to certify that **Sonali Khan** of **Presidency University, Kolkata, West Bengal** presented a poster at the National Virtual Conference (NVC-2021) on **Genomics to Phenomics: A New Horizon in Plant Science Research** held on 28th February and 1st March, 2021.

Prof. Binay Chaubey
Head, Department of Botany,
University of Calcutta

Dr. Maumita Bandyopadhyay, Dr. Sudipta Ray, Dr. Soumitra Paul
Conveners,
National Virtual Conference 2021

First page of published manuscript

Archives of Biochemistry and Biophysics 731 (2022) 109446

Contents lists available at ScienceDirect

Archives of Biochemistry and Biophysics

journal homepage: www.elsevier.com/locate/yabbi

A CobB like sirtuin in *Oryza sativa indica* regulates the mitochondrial machinery under stress conditions

Sonali Khan, Nilabhra Mitra, Sanghamitra Dey *

Department of Life Sciences, Presidency University, 86/1 College Street, Kolkata, West Bengal, 700073, India

ARTICLE INFO

Keywords:
Plant sirtuin
Deacetylation
CobB-like protein
Mitochondria
Stress response
Metabolic regulation

ABSTRACT

Sirtuins are ubiquitous in nature and are known to play an important role as metabolic regulators. In plants, these NAD^+ dependent deacetylases are not well characterized. In this study, we are reporting a new member of sirtuin in *Oryza sativa indica*. OsCobB shares approx. 89% sequence identity with bacterial sirtuin, a class III sirtuin member. This protein is mostly present in mitochondria with trace amounts in the nucleus. It can physically interact with histones H3 and H4 and can specifically deacetylate histone H3 at Lys^9 and Lys^{18} positions. In mitochondria, acetyl coA synthetase (ACS) and isocitrate dehydrogenase 2 (IDH2) are the targets for its deacetylation. This removal of acetyl group is the mode of regulation under certain stress conditions. Thus, this is the first mitochondrial CobB targeting important plant machinery under changing growth environment. The OsCobB deacetylase activity is not majorly affected by its products, nicotinamide and ADP ribose but are sensitive to certain metal ions like Fe^{2+} and Mg^{2+}. In contrast to some class III members, it does not have any ADP ribosyl transferase activity. In response to abiotic stress conditions like dehydration and low temperature, this enzyme can also mobilize to the nucleus to regulate the plant metabolism.

1. Introduction

Plant proteins undergo post translational modifications (PTM) in response to environmental changes. PTM provides a wide range of protein diversity in this complex plant system to sustain changes in the surrounding environment. The process of acetylation/deacetylation are one of such modifications. Unravelling the mysteries of the PTM's involvement in these complex mechanisms is highly intriguing.

The class III HDAC member, sirtuins are classified into four major classes (I-IV), depending on their amino acid sequence in the core domains as well as cellular localization in both prokaryotes and eukaryotes [1]. Among mammalian sirtuins, SIRT1, 2, and 3 are class I sirtuins, having high homology to the yeast Sir2 and proteins such as Hst1, and Hst2, and exhibit robust deacetylase activity [1]. Class II sirtuins, including mammalian SIRT4, have no detectable deacetylase activity and instead show weak ADP ribosyltransferase activity [1,2]. Class III sirtuin, SIRT5 has weak deacetylase activity with several other lysine deacylase activities like desuccinylase, demalonylase *etc.* [3]. Most of the bacterial sirtuins also belong to this class. Few of the examples are Af1 from *Archaeoglobus fulgidus* (CobB1) [4], CobB from *Escherichia coli* [5] and *Salmonella enterica* [6], pfsirt2A from *Plasmodium falciparum* [7]. Class IV sirtuins have both ADP ribosyltransferase and deacetylase activity (SIRT6 and SIRT7) [8,9]. Collectively, sirtuins play important roles in regulating genomic stability, energy metabolism, and stress resistance in a variety of organisms [10]. SIRT1, 6 and 7 are nuclear proteins and it is strongly evident that SIRT1 and 6 are linked to stress responses and related aging processes [8,11,12]. On the other hand, SIRT3, 4 and 5 are mitochondrial proteins involved in regulation of energy metabolism and cellular impairment during the aging process [1–3,13–16]. Thus, human sirtuins are targets of major therapeutic studies.

In comparison, plant sirtuins have not been studied in great detail. Two genes coding for sirtuins were identified in *Vitis vinifera*, namely VvSRT1, localized in the nucleus and VvSRT2, localized in both mitochondria and chloroplast [17,18]. VvSRT1 is noted to play a role in plant development whereas VvSRT2 is involved in maintaining the chromatin structure and regulation of gene transcription, indirectly linked to plant photosynthesis as well as leaf senescence. Two sirtuin genes have also

Abbreviations: PTM, post translational modification; HDAC, histone deacetylase; NAD^+, nicotinamide adenine dinucleotide; $NADP^+$, nicotinamide adenine dinucleotide phosphate; ADPr, ADP ribose; NAM, nicotinamide; ACS, acetyl CoA Synthetase; IDH2, isocitrate dehydrogenase 2; GAPDH, glyceraldehyde phosphate dehydrogenase; AOX1/2, alternative oxidase 1/2; FNR, ferrodoxin NADP reductase.

* Corresponding author.
E mail address: sdey.dbs@presiuniv.ac.in (S. Dey).

https://doi.org/10.1016/j.abb.2022.109446
Received 18 April 2022; Received in revised form 11 October 2022; Accepted 15 October 2022
Available online 22 October 2022
0003-9861/© 2022 Elsevier Inc. All rights reserved.